EM-Neuro Modeling Across Scales for Bioelectronic Medicine

Lecture 8: Neural Mass & Whole-Brain Models; Hybridization

Esra Neufeld[*] and Taylor Newton[*†]

[*]IT'IS Foundation for Research on Information Technologies in Society

[†]Integrated Systems Laboratory, ETH Zurich

Outline for Today

- From spikes to populations: Mean-field reduction, Wilson–Cowan, Jansen–Rit, the NMM zoo
- Bifurcation analysis & stochastic dynamics: Phase plane, bifurcation types, hysteresis, stochastic NMMs, SDE numerics
- Epilepsy as a dynamical disease: Seizures as bifurcations, Saggio taxonomy, Epileptor, Virtual Epileptic Patient, closed-loop control
- Whole-brain models: Structural connectivity, region- and surface-based models, The Virtual Brain, subject-specific predictions
- Hybridization: Bridging scales; the IT'IS/Jirsa pipeline for personalized non-invasive brain stimulation [1]
- Exercise session: Prof. Niels Kuster guest lecture: “Coexistence & Synergy: Basic Research, Innovations, and Spin-Offs at Z43”

Course Outline

DATE	LECTURE THEME
19.02	Motivation, logistics & tooling (EN, TNE)
26.02	Ion channels & membranes (EN)
05.03	Axon models, activating functions & electrical stimulation (EN)
12.03	EM field simulation fundamentals & coupled EM-neuro workflows (EN)
19.03	Peripheral nerves & interfaces for bioelectronic medicine (EN)
26.03	Spinal cord stimulation for neuroprosthetics and pain management & low-frequency exposure safety (TNE)
02.04	Morphology, synapses, microcircuits; point vs spiking networks (TNE)
09.04	No class: Easter break
16.04	Neural mass & whole brain models; hybridization (TNE)
23.04	Recording modalities, signal content & the reciprocity theorem (TNE)
30.04	Non invasive brain stimulation & temporal interference (TNE)
07.05	Image based/personalized treatment planning and optimization (EN)
14.05	No class: Ascension Day
21.05	Verification, validation, UQ, and reproducibility (EN)
28.05	Project presentations & synthesis (EN, TNE)

Room: ETZ E7

13:15-14:00 Lecture

14:00-14:15 Break

14:15-15:00 Lecture

15:00-15:15 Break

15:15-16:00 Exercise

Recorded Lectures & Course Material

Provided Here

Exercise Outline

DATE	EXERCISE THEME
19.02	"Hello Neuron": integrate-and-fire in Python/NEURON
26.02	Point neuron phase portrait; basic time integration numerics
05.03	Recruitment prediction for myelinated axon using AF/GAF
12.03	EM (FEM) modeling of transcranial brain stimulation
19.03	Stimulation selectivity and signal content modeling for nerve interfaces
26.03	Guest (SCS – NeuroRestore)
02.04	Mini project work
09.04	No class: Easter break
16.04	Guest: Prof. Niels Kuster (Neuromodulation Spin-Off – Z43)
23.04	Mini project work
30.04	Guest (NIBS – Kinderspital)
07.05	Mini project work
14.05	No class: Ascension Day
21.05	Mini project work
28.05	Project presentations

Room: ETZ E7

13:15-14:00 Lecture

14:00-14:15 Break

14:15-15:00 Lecture

15:00-15:15 Break

15:15-16:00 Exercise

Learning Objectives

- Motivate the step from spiking networks to neural mass models (NMMs) and state the assumptions of mean-field reduction
- Write down the Wilson-Cowan [2] and Jansen-Rit [3] equations and interpret their parameters biophysically
- Apply phase-plane & bifurcation analysis to a two-population rate model; identify bifurcations [4]
- Explain how noise drives transitions between coexisting attractors; integrate stochastic NMMs with Euler–Maruyama and Milstein schemes [5]
- Describe epilepsy as a dynamical disease and outline the Epileptor / Virtual Epileptic Patient framework [6, 7, 8]
- Describe how structural connectivity and region-based NMMs combine into whole-brain models [9]
- Articulate the hybridization concept: coupling biophysically detailed local models with phenomenological whole-brain NMMs for stimulation prediction [1]

Recommended Reading

- Wilson & Cowan (1972). Excitatory and inhibitory interactions in localized populations of model neurons. *Biophys. J.* 12:1–24 [2]
- Jansen & Rit (1995). Electroencephalogram and visual evoked potential generation in a mathematical model of coupled cortical columns. *Biol. Cybern.* 73:357–366 [3]
- Deco, Jirsa, Robinson, Breakspear & Friston (2008). The dynamic brain: from spiking neurons to neural masses and cortical fields. *PLoS Comput. Biol.* 4:e1000092 [9]
- Jirsa, Stacey, Quilichini, Ivanov & Bernard (2014). On the nature of seizure dynamics. Brain 137:2210–2230 [6]
- Saggio et al. (2020). A taxonomy of seizure dynamotypes. *eLife* 9:e55632 [10]
- Sanz Leon et al. (2013). The Virtual Brain: a simulator of primate brain network dynamics. *Front. Neuroinform.* 7:10 [11]
- Karimi et al. (2025). Precision non-invasive brain stimulation: an in silico pipeline. *J. Neural Eng.* 22:026061 [1]
- Higham (2001). An algorithmic introduction to numerical simulation of SDEs. *SIAM Rev.* 43:525–546 [5]

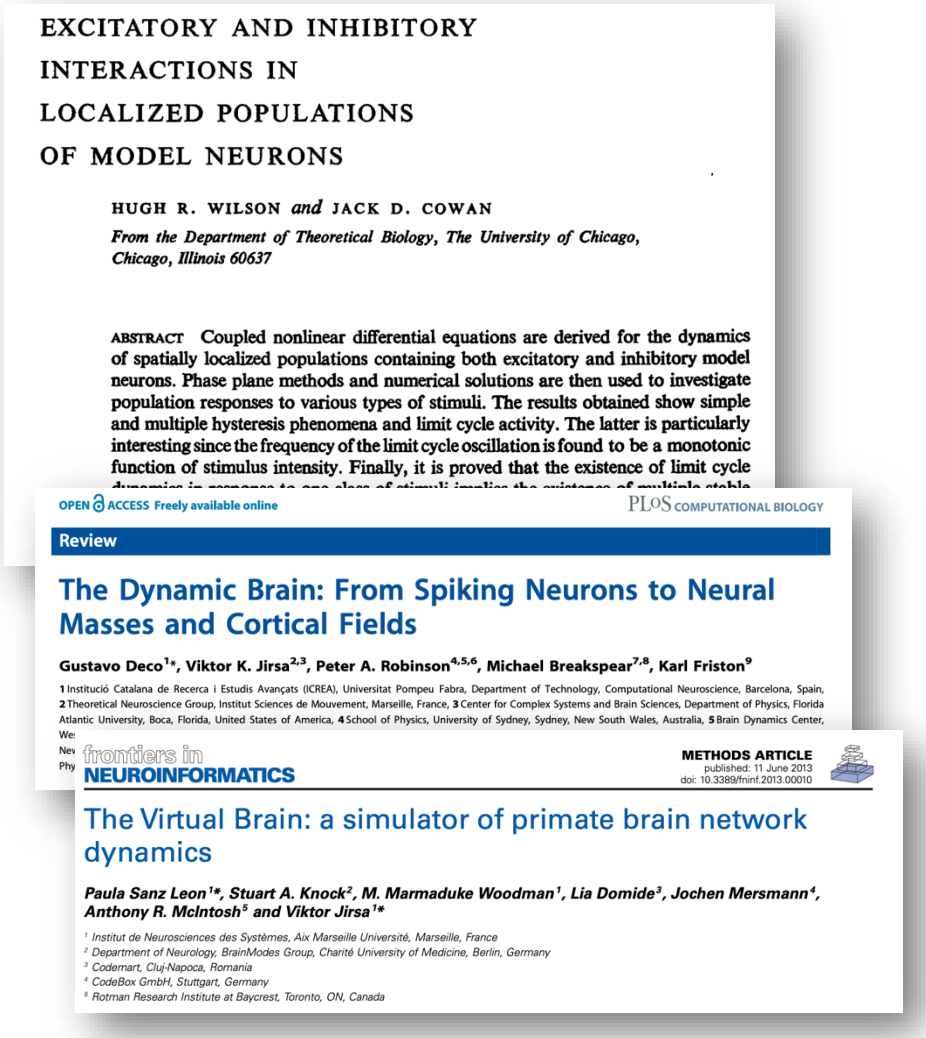

EXCITATORY AND INHIBITORY INTERACTIONS IN LOCALIZED POPULATIONS OF MODEL NEURONS

HUGH R. WILSON *and* JACK D. COWAN

From the Department of Theoretical Biology, The University of Chicago, Chicago, Illinois 60637

ABSTRACT Coupled nonlinear differential equations are derived for the dynamics of spatially localized populations containing both excitatory and inhibitory model neurons. Phase plane methods and numerical solutions are then used to investigate population responses to various types of stimuli. The results obtained show simple and multiple hysteresis phenomena and limit cycle activity. The latter is particularly interesting since the frequency of the limit cycle oscillation is found to be a monotonic function of stimulus intensity. Finally, it is proved that the existence of limit cycle

OPEN ACCESS Freely available online

PLOS COMPUTATIONAL BIOLOGY

Review

The Dynamic Brain: From Spiking Neurons to Neural Masses and Cortical Fields

Gustavo Deco[1]*, Viktor K. Jirsa[2,3], Peter A. Robinson[4,5,6], Michael Breakspear[7,8], Karl Friston[9]

1 Institució Catalana de Recerca i Estudis Avançats (ICREA), Universitat Pompeu Fabra, Department of Technology, Computational Neuroscience, Barcelona, Spain, 2 Theoretical Neuroscience Group, Institut Sciences de Mouvement, Marseille, France, 3 Center for Complex Systems and Brain Sciences, Department of Physics, Florida Atlantic University, Boca, Florida, United States of America, 4 School of Physics, University of Sydney, Sydney, New South Wales, Australia, 5 Brain Dynamics Center,

frontiers in NEUROINFORMATICS

METHODS ARTICLE
published: 11 June 2013
doi: 10.3389/fninf.2013.00010

The Virtual Brain: a simulator of primate brain network dynamics

Paula Sanz Leon[1], Stuart A. Knock[2], M. Marmaduke Woodman[1], Lia Domide[3], Jochen Mersmann[4], Anthony R. McIntosh[5] and Viktor Jirsa[1]**

[1] Institut de Neurosciences des Systèmes, Aix Marseille Université, Marseille, France
[2] Department of Neurology, BrainModes Group, Charité University of Medicine, Berlin, Germany
[3] Codemart, Cluj-Napoca, Romania
[4] CodeBox GmbH, Stuttgart, Germany
[5] Rotman Research Institute at Baycrest, Toronto, ON, Canada

Outline for Today

- **From spikes to populations: Mean-field reduction, Wilson–Cowan, Jansen–Rit, the NMM zoo**
- Bifurcation analysis & stochastic dynamics: Phase plane, bifurcation types, hysteresis, stochastic NMMs, SDE numerics
- Epilepsy as a dynamical disease: Seizures as bifurcations, Saggio taxonomy, Epileptor, Virtual Epileptic Patient, closed-loop control
- Whole-brain models: Structural connectivity, region- and surface-based models, The Virtual Brain, subject-specific predictions
- Hybridization: Bridging scales; the IT'IS/Jirsa pipeline for personalized non-invasive brain stimulation [1]
- Exercise session: Prof. Niels Kuster guest lecture: “Coexistence & Synergy: Basic Research, Innovations, and Spin-Offs at Z43”

Why Go Beyond Spiking Networks?

Recall from W07: even a single cortical column (~31k neurons) is already computationally demanding (Blue Brain Project).

Whole brain: ~86 × 10^9 neurons [12]; ~10^2–10^3 parcellated regions, or ~10^4–10^5 vertices in high-resolution surface models (see Part IV) [13].

Three reasons to step up a level:

- Computational tractability — neural mass models (NMMs) reduce each region to 2–6 ODEs; whole-brain models become feasible on a laptop
- Analytical tractability — bifurcation, stability, and control-theoretic tools apply directly → predictions about state transitions (seizures, sleep, anesthesia) without simulation [4]
- Direct link to macroscopic observables — NMM output (mean postsynaptic potential: PSP, population rate) maps naturally to EEG/fMRI → model fitting and clinical validation [9]

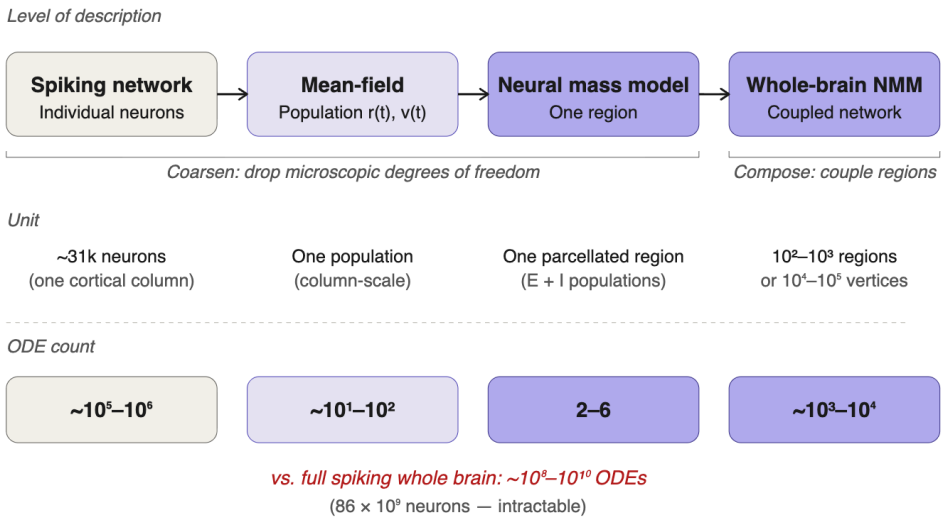

The same 'what is lost' logic from W07 applies one level up.

From Spikes to Rates

Describe N neurons by a few macroscopic variables (mean firing rate r(t), mean membrane potential v(t)) instead of N individual traces.

Three assumptions for validity:

- Large N — thermodynamic limit; fluctuations scale as $1/\sqrt{N}$
- Statistical homogeneity — shared parameters within a population
- Weak pairwise correlations — sparse random connectivity; each neuron sees ~independent input

Preserved:

- Mean firing rates
- Oscillation frequencies
- Stability boundaries
- Qualitative state transitions

Lost:

- Individual spike times
- Precise pairwise correlations
- Fine within-population spatial structure

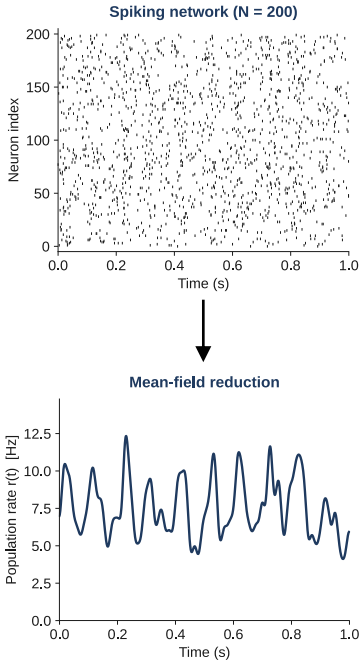

The Wilson-Cowan Equations

Two-population rate model [2]:

$$\tau_I \frac{dI}{dt} = -I + S_I(w_{EI}E - w_{II}I + Q)$$

$$\tau_E \frac{dE}{dt} = -E + S_E(w_{EE}E - w_{IE}I + P)$$

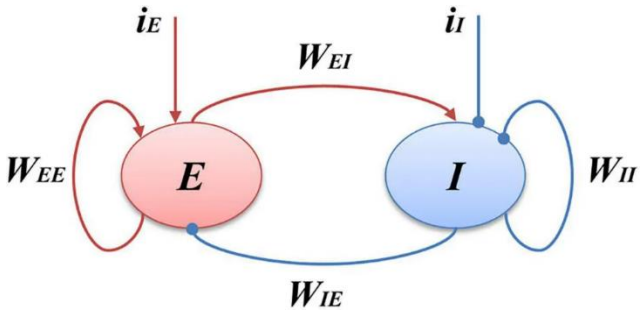

Li X et al. (2022). *Front. Syst. Neurosci.* 16:723237. doi: 10.3389/fnsys.2022.723237

E(t), I(t): population-averaged activity (firing-rate-like).
$\tau_E, \tau_I \approx$ 5–20 ms (typically $\tau_I \gtrsim \tau_E$) · w_{jk}: connection weights · $P_{E,I}$: external drive.

The sigmoid — not arbitrary:

$$S(x) = \frac{1}{1 + e^{-a(x-\theta)}}$$

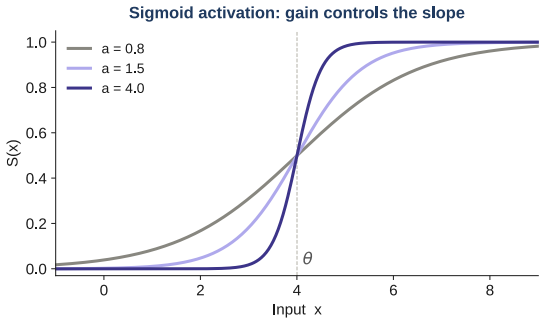

- E(t), I(t): fraction of active excitatory / inhibitory neurons
- $w_{EE}, w_{IE}, w_{EI}, w_{II}$: connection weights (E→E, I→E, E→I, I→I)
- P, Q: external input drives
- τ_E, τ_I: population time constants
- a, θ: sigmoid gain and threshold (can differ between E and I)

Inhibition-stabilized network (ISN) regime from W07 corresponds to a specific (w_{EI} ,w_{EE}) region — today we map the full landscape [15, 4].

- Arises from the distribution of firing thresholds across the population
- Identical thresholds → step function; heterogeneity smooths it into a sigmoid
- Gain a = inverse width of the threshold distribution; midpoint θ = population median threshold

The Jansen-Rit Model

Architecture: pyramidal cells + excitatory interneurons + inhibitory interneurons — a minimal cortical column [3].

Second-order PSP kernels rewritten as 6 first-order ODEs:

$$\dot{y}_5 = BbC_4 \cdot S(C_3 y_0) - 2b y_5 - b^2 y_2$$
$$\dot{y}_2 = y_5$$
$$\dot{y}_4 = Aa\{p(t) + C_2 \cdot S(C_1 y_0)\} - 2a y_4 - a^2 y_1$$
$$\dot{y}_1 = y_4$$
$$\dot{y}_3 = Aa \cdot S(y_1 - y_2) - 2a y_3 - a^2 y_0$$
$$\dot{y}_0 = y_3$$

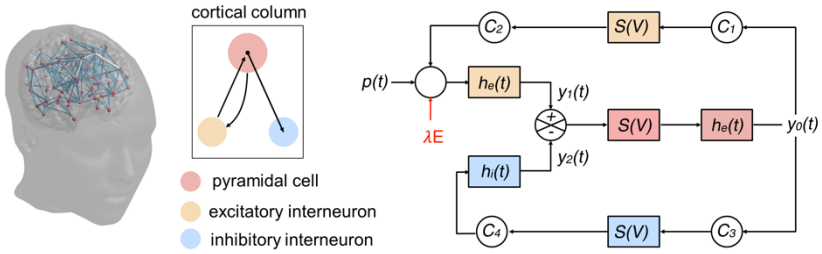

y_0: pyramidal PSP y_1: excitatory input to pyramidal y_2: inhibitory input to pyramidal ***$y_1 - y_2$: net source PSP on pyramidal (OUTPUT)***

Alpha regime (~10 Hz) reproduces resting EEG [3, 16]

Standard parameters [3]

- A = 3.25 mV, a = 100 s^{-1}
- B = 22 mV, b = 50 s^{-1}
- C_1 = C, C_2 = 0.8 C
- C_3 = C_4 = 0.25 C
- C = 135
- p(t): extrinsic input (noise or drive)

$$S(v) = \frac{2e_0}{1 + \exp\big(r(v_0 - v)\big)},$$
$$e_0 = 2.5\ \mathrm{s}^{-1},$$
$$v_0 = 6\ \mathrm{mV},$$
$$r = 0.56\ \mathrm{mV}^{-1}$$

EEG-like observable

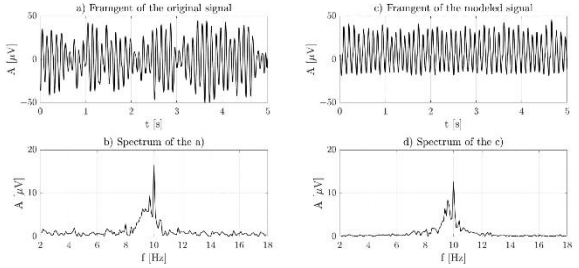

Image: Łysiak, A.; Paszkiel, S. *Appl. Sci.* **2021**, *11*, 677

The Jansen-Rit Model

Architecture: pyramidal cells + excitatory interneurons + inhibitory interneurons — a minimal c

Second-ord

$$\dot{y}_5 = BbC_4$$
$$\dot{y}_2 = y_5$$
$$\dot{y}_4 = Aa\{p$$
$$\dot{y}_1 = y_4$$
$$\dot{y}_3 = Aa \cdot S$$
$$\dot{y}_0 = y_3$$

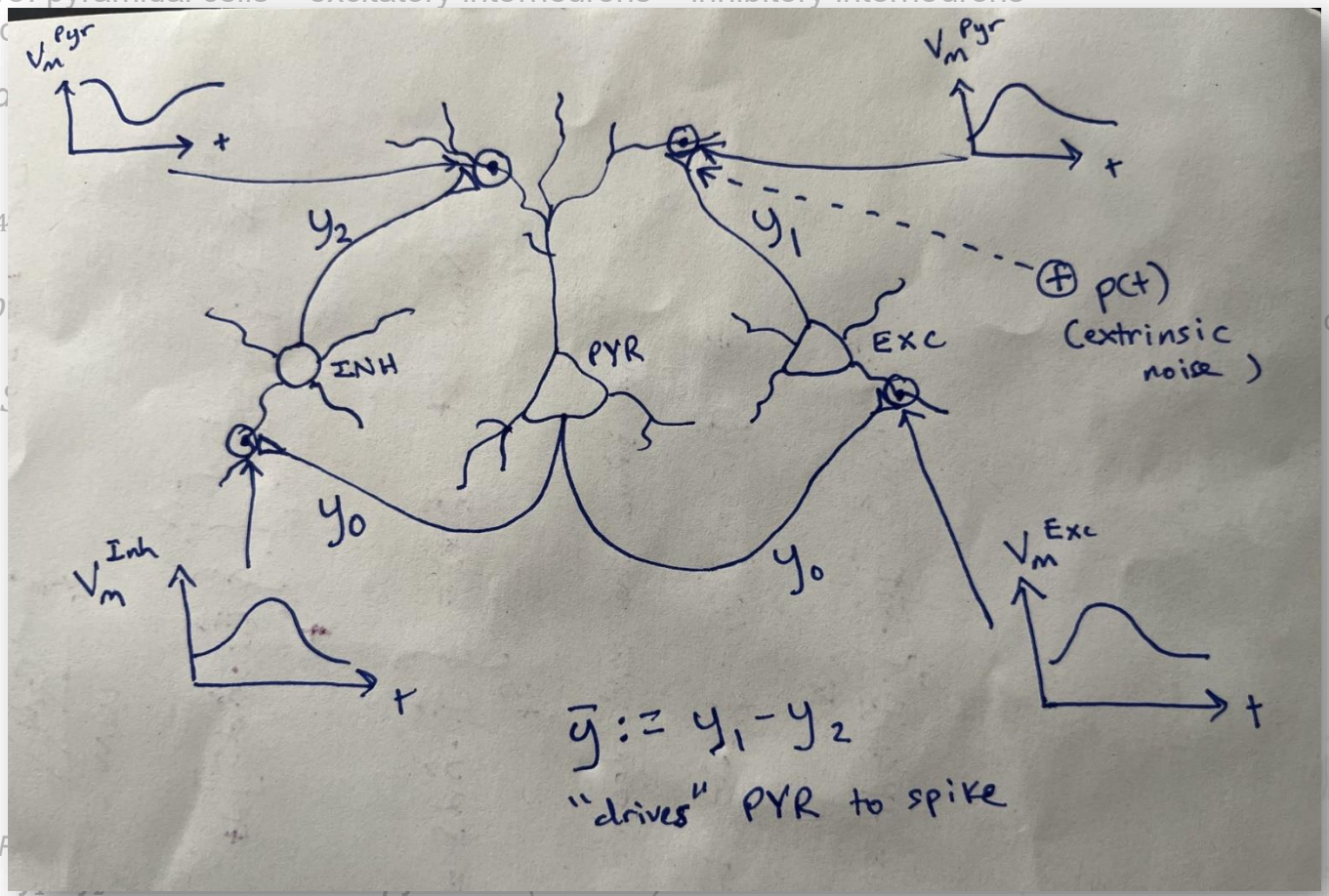

y_0: pyramidal P to pyramidal

Alpha regime (~10 Hz) reproduces resting EEG [3, 16]

Image: Łysiak, A.; Paszkiel, S. *Appl. Sci.* **2021**, *11*, 677

W-C vs. J-R: When Does it Matter?

Feature	Wilson–Cowan	Jansen–Rit
Variables	2 (E, I rates)	6 (3 PSPs + 3 derivatives)
Synaptic kernel	1st-order exponential decay	2nd-order alpha function
PSP waveform	No explicit PSP kernel	Realistic rise / fall
Oscillations	Only in certain parameter regimes	More readily supports alpha-range oscillations under standard parameterizations
Analytical tractability	High — 2D phase plane	Moderate — 6D but feasible
EEG output	Not explicit	$y_1 - y_2$ EEG-like

When to use which:

- Wilson–Cowan: bifurcation analysis, minimal models, theoretical insight
- Jansen–Rit: realistic EEG spectra, forward modeling, physiologically interpretable columns for whole-brain simulation [9]

The NMM Zoo

*Wilson–Cowan (**W-C**) and Jansen–Rit (**J-R**) are the canonical starting points — the field branches from there.*

- Freeman K-sets (1975) — hierarchical architecture (KO → KI → KII → KIII); asymmetric sigmoids, chaotic dynamics for pattern recognition [17]
- Wendling et al. (2002) — adds fast GABA_A dendritic inhibition to Jansen–Rit (8–10 ODEs); reduced dendritic inhibition → epileptic fast activity (20–100 Hz). Returns in Part III [14]
- David & Friston (2003) — multiple subpopulations with distinct kinetics → multimodal spectra (α + γ). Foundation for Dynamic Causal Modelling (DCM) [18]
- Montbrió, Pazó & Roxin (2015) — next-generation NMM: exact mean-field reduction, tracks synchrony [14]
- Liley et al. (2002) — conductance-based synapses with reversal potentials (more biophysically grounded than J-R); later work (Steyn-Ross, Bojak, Dafilis) explores rich dynamics including anesthesia-related state transitions [19]

Next-generation NMMs — Montbrió, Pazó & Roxin (2015) [14]: exact mean-field reduction for quadratic integrate-and-fire (QIF) neurons. Two ODEs track r(t) and v(t) → captures synchrony. In the slow-synapse limit, formally equivalent to a Wilson–Cowan-like firing-rate description.

All share the same ingredients: populations + sigmoid + synaptic kernels + connectivity weights.

Part I Summary: The Abstraction Ladder Updated

From W07 we had:

Multi-compartment Hodgkin-Huxley (HH) → Point neurons → Spiking-network mean-field (Brunel)

Today we extend it:

… → Neural mass models (W-C, J-R) → Neural field models

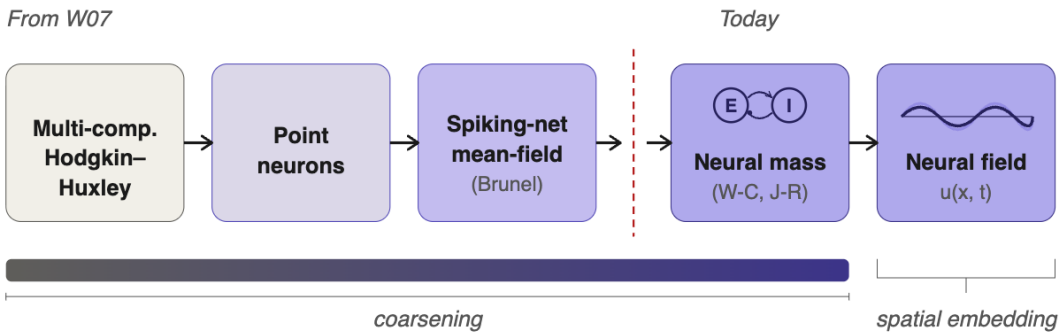

Coarsening (HH → NMM)

- Reduced computational cost
- Broader temporal scale
- Loss of biophysical specificity

Spatial embedding (NMM → field)

- Continuous spatial coordinate x
- Pattern formation (waves, bumps)
- Cost increases with resolution

The question for the rest of the lecture: what can we DO with NMMs that we couldn't do (easily) with spiking models? Answer: bifurcation analysis, clinical prediction, whole-brain simulation.

Outline for Today

- From spikes to populations: Mean-field reduction, Wilson–Cowan, Jansen–Rit, the NMM zoo
- **Bifurcation analysis & stochastic dynamics: Phase plane, bifurcation types, hysteresis, stochastic NMMs, SDE numerics**
- Epilepsy as a dynamical disease: Seizures as bifurcations, Saggio taxonomy, Epileptor, Virtual Epileptic Patient, closed-loop control
- Whole-brain models: Structural connectivity, region- and surface-based models, The Virtual Brain, subject-specific predictions
- Hybridization: Bridging scales; the IT'IS/Jirsa pipeline for personalized non-invasive brain stimulation [1]
- Exercise session: Prof. Niels Kuster guest lecture: “Coexistence & Synergy: Basic Research, Innovations, and Spin-Offs at Z43”

Phase-Plane Analysis of Wilson-Cowan

Recall W02: we analyzed the Hodgkin–Huxley equations using nullclines and fixed points. Wilson–Cowan is two-dimensional: the same graphical tools apply, with 'E' as the fast 'voltage-like' variable and 'I' as the slow 'recovery-like' variable (when $\tau_I > \tau_E$).

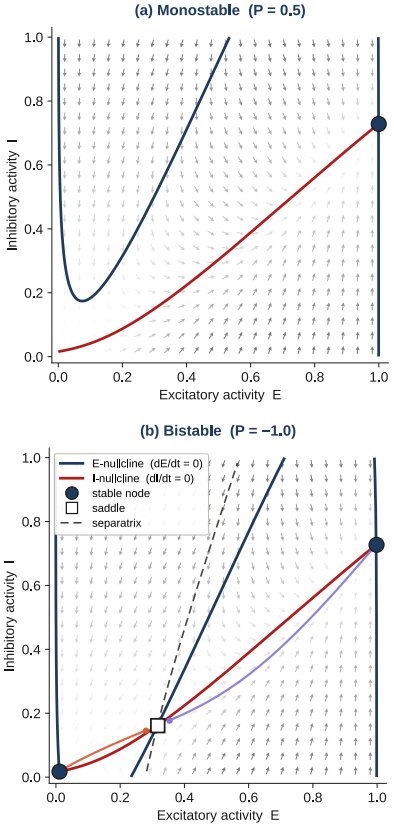

Nullclines and fixed points:

- E-nullcline (dE/dt = 0): curve in the (E, I) plane where excitation balances decay
- I-nullcline (dI/dt = 0): inhibition balances decay
- Fixed points = intersections. Depending on parameters, one can obtain multiple fixed points — often 1 or 3, and in some formulations even 5

Jacobian at a fixed point:

$$J = \begin{bmatrix} (-1 + w_{EE}S'_E)/\tau_E & (-w_{EI}S'_E)/\tau_E \\ (w_{IE}S'_I)/\tau_I & (-1 - w_{II}S'_I)/\tau_I \end{bmatrix}$$

Note: S'_E ,S'_I are evaluated at the sigmoid INPUT at the fixed point (i.e. w.r.t. the argument $x = w_{EE}E * -w_{EI}I * +P_E$,(not w.r.t. E or I directly.

Stability classification:

- Stable when tr(J) < 0 and det(J) > 0
- Saddle when det(J) < 0
- Unstable focus (potential limit cycle) when tr(J) > 0 and det(J) > 0

Phase-Plane Analysis of Wilson-Cowan

Recall W02: we analyzed the Hodgkin–Huxley equations using nullclines and fixed points. Wilson–Cowan is two-dimensional: the same graphical tools apply, with 'E' as the fast 'voltage-like' variable and 'I' as the slow 'recovery-like' variable (when $\tau_I > \tau_E$).

Nullclines and fixed points:

- E-nullcline (dE/dt = 0): curve in the (E, I) plane where excitation balances decay
- I-nullcline (dI/dt = 0): inhibition balances decay
- Fixed points = intersections. Depending on parameters, one can obtain multiple fixed points — often 1 or 3, and in some formulations even 5

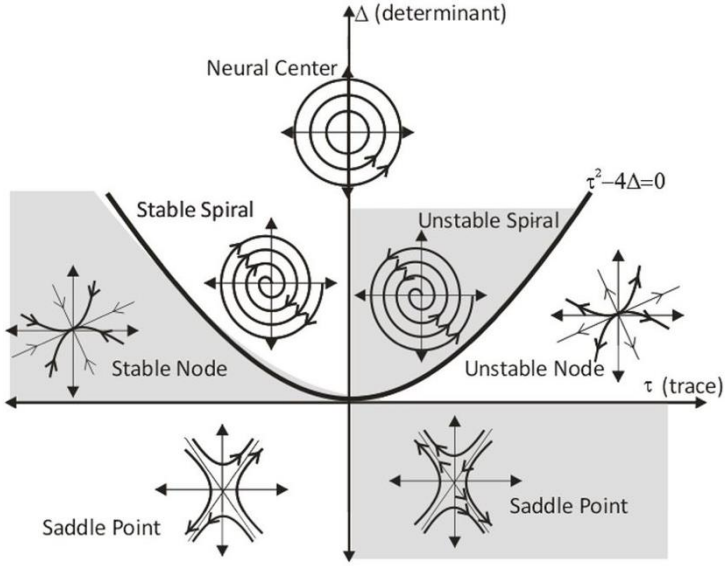

Erbaş, K. C. (2022) Chaos Theory and Applications, 4(1), 37-44

Jacobian at a fixed point:

$$J = \begin{bmatrix} (-1 + w_{EE}S'_E)/\tau_E & (-w_{EI}S'_E)/\tau_E \\ (w_{IE}S'_I)/\tau_I & (-1 - w_{II}S'_I)/\tau_I \end{bmatrix}$$

Note: S'_E, S'_I are evaluated at the sigmoid INPUT at the fixed point (i.e. w.r.t. the argument $x = w_{EE}E * -w_{EI}I * +P_E$), not w.r.t. E or I directly.

Stability classification:

- Stable when tr(J) < 0 and det(J) > 0
- Saddle when det(J) < 0
- Unstable focus (potential limit cycle) when tr(J) > 0 and det(J) > 0

Bifurcation Types that Govern NMM Dynamics

Four key bifurcation types, each producing a qualitatively distinct dynamical phenomenon [4]:

Saddle-node (fold) → Bistability

Two fixed points (stable node + saddle) collide and annihilate. One eigenvalue passes through zero. Normal form: $\dot{x} = \mu + x^2$. In NMMs: cortical up/down states, working memory.

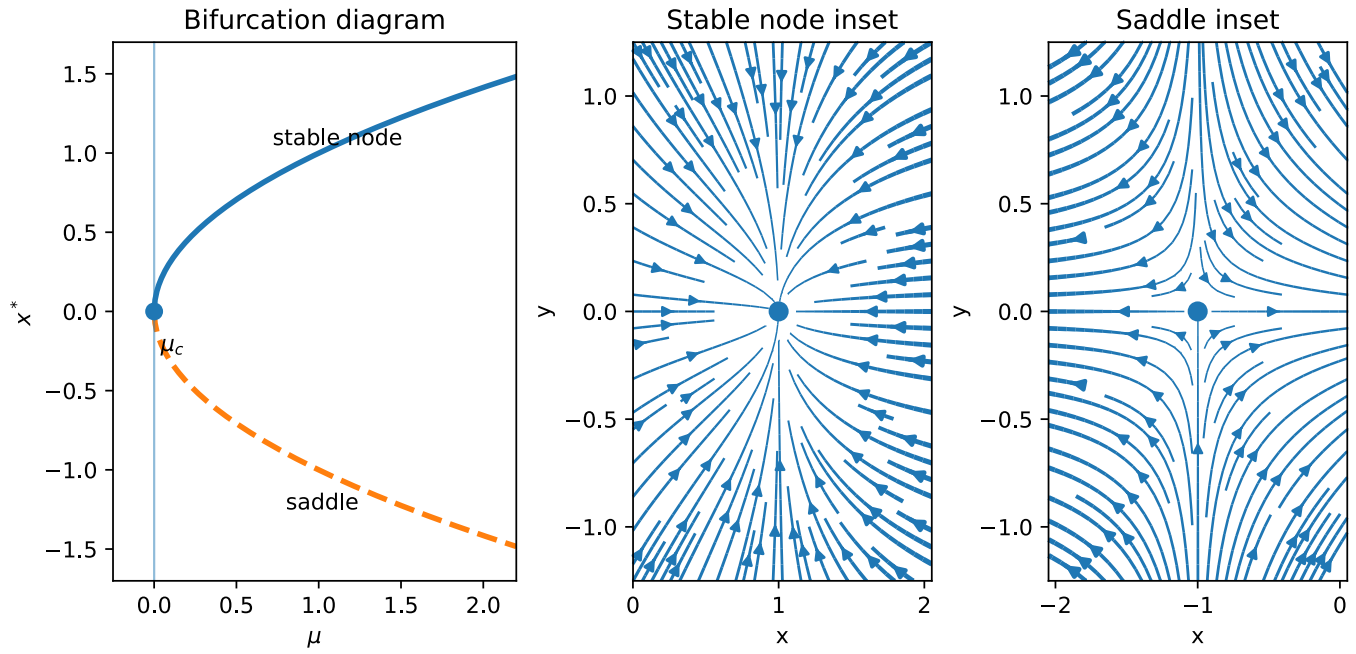

Bifurcation Types that Govern NMM Dynamics

Four key bifurcation types, each producing a qualitatively distinct dynamical phenomenon [4]:

Hopf → Oscillation onset

Complex eigenvalues cross the imaginary axis. Supercritical: limit cycle grows smoothly from zero amplitude. Subcritical: abrupt jump + hysteresis. Key organizer of α and γ rhythms.

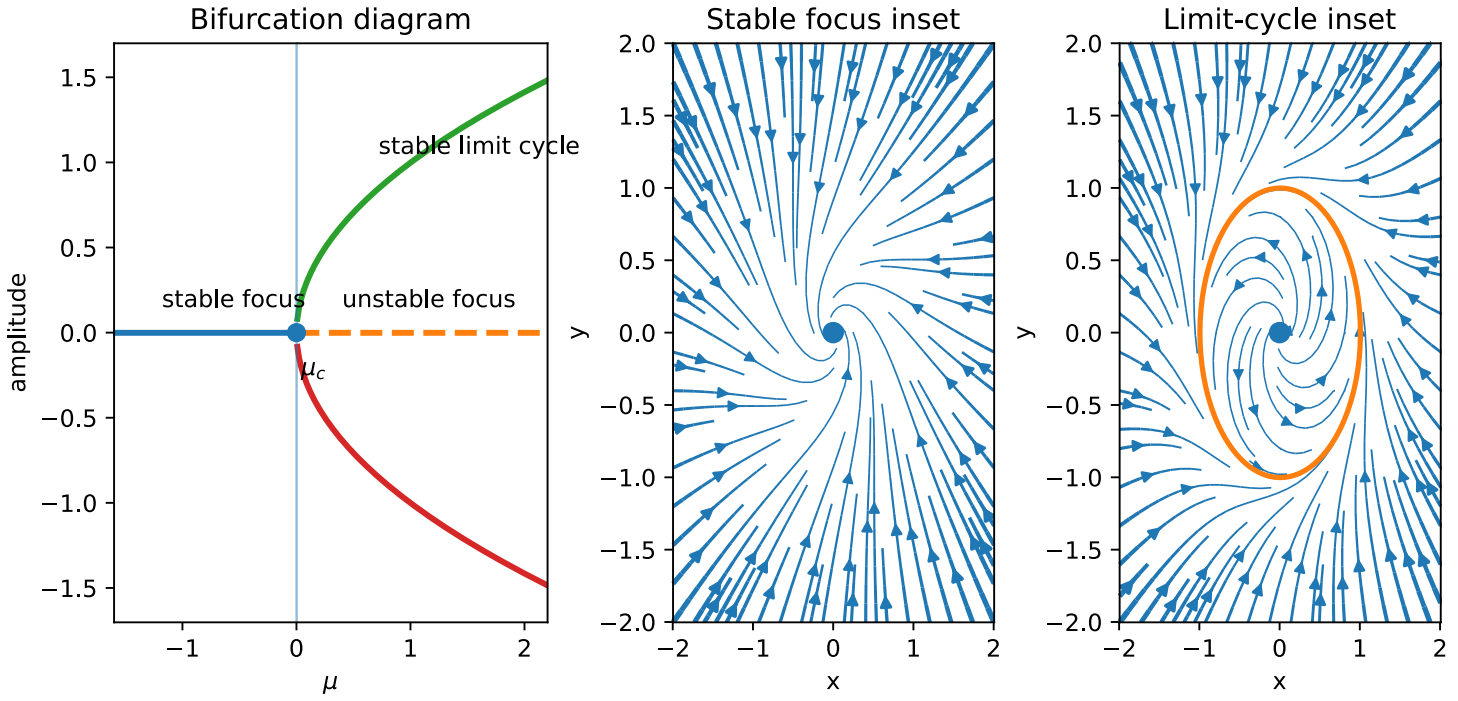

Bifurcation Types that Govern NMM Dynamics

Four key bifurcation types, each producing a qualitatively distinct dynamical phenomenon [4]:

Saddle-node on invariant circle (SNIC) → Excitable to oscillatory

A saddle/stable node collide on a limit cycle. Below threshold: excitable (pulse response). Above threshold: frequency approaches zero continuously at onset, allowing arbitrarily low firing rates near threshold. Encodes stimulus intensitv as rate.

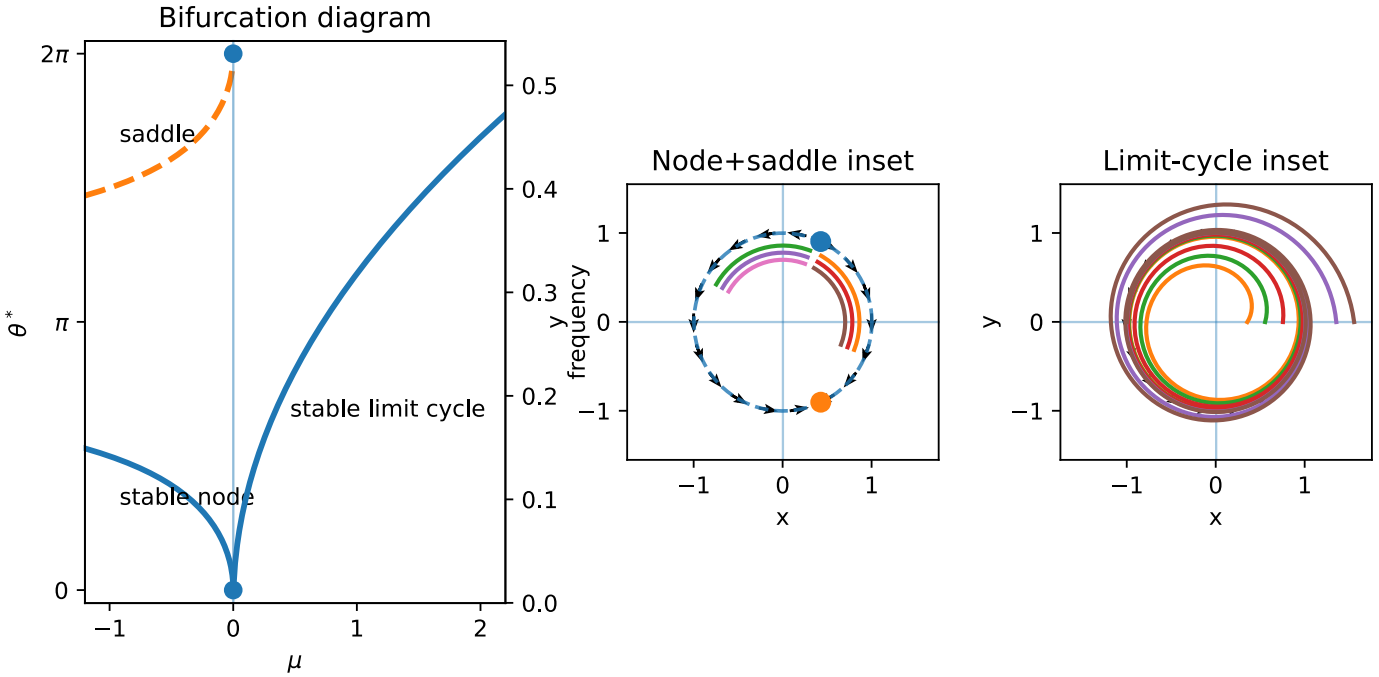

Bifurcation Types that Govern NMM Dynamics

Four key bifurcation types, each producing a qualitatively distinct dynamical phenomenon [4]:

Homoclinic orbit → Bursting

A limit cycle collides with a saddle point, period → ∞ logarithmically. Combined with a slow variable, produces alternating bursting and quiescence. Returns in the Epileptor (Part III).

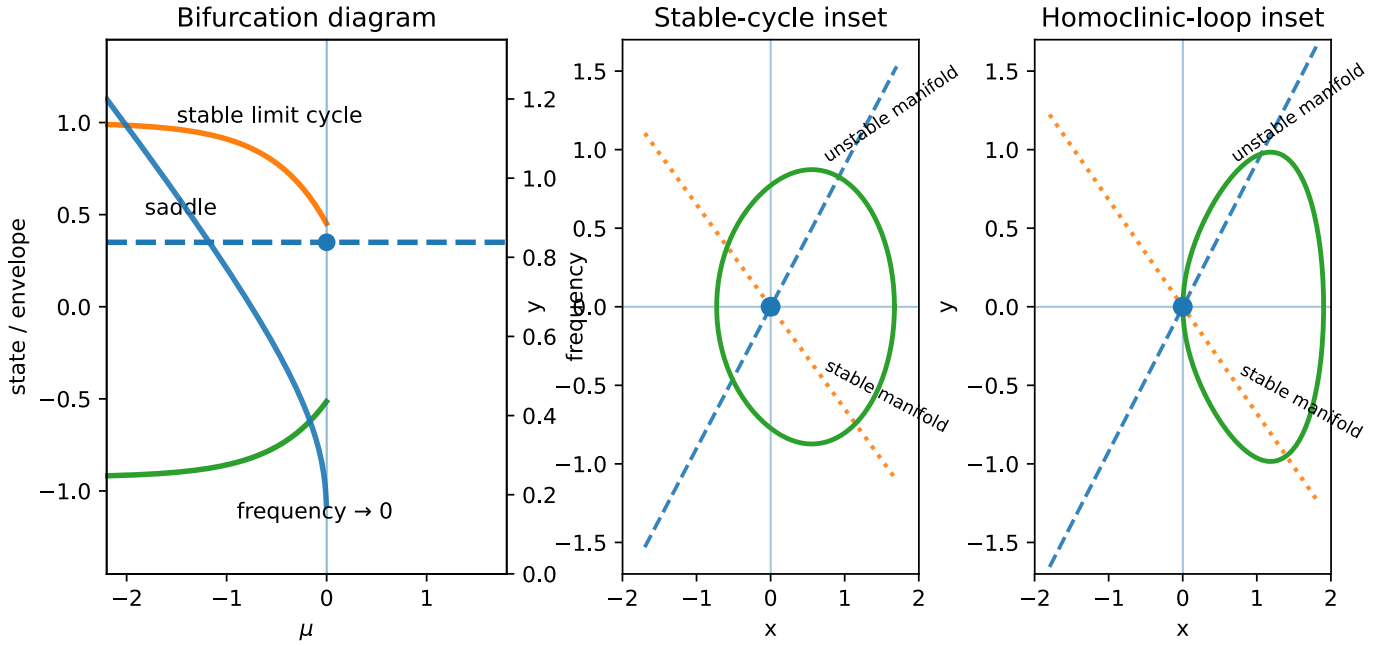

Bifurcation Diagram: Sweeping External Drive

One point organizes the landscape

- In two-parameter space (P, c_3), the SN, AH, and SHO curves all emanate from a single codimension-2 point — the Bogdanov–Takens (BT) point
- BT is a normal-form organizing center: its local unfolding dictates which bifurcation curves exist nearby and how they meet
- The plane is partitioned into qualitatively distinct dynamical regimes — each region has a different fixed-point / limit-cycle structure

Why this matters

- 2D portrait compresses the entire qualitative repertoire of the model into a single map
- Knowing where you are relative to BT tells you which transitions are reachable by small parameter changes

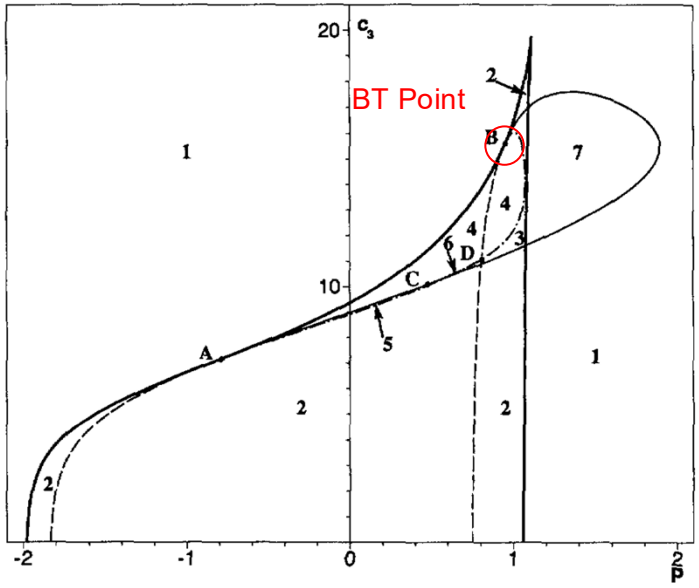

Image: Borisyuk & Kirillov 1992 [20]

Hysteresis and Multistability: Why it Matters (Clinically)

When the system has two coexisting stable states for the same parameter values, its HISTORY determines its current state. A transient perturbation can flip the system between attractors permanently.

Clinical mappings (dynamical-systems interpretations):

- Cortical up / down states — alternation between depolarized (up) and hyperpolarized (down) states during slow-wave sleep and anesthesia can be modeled as noise-driven transitions between two attractors [21]
- Seizure onset is often interpreted as a parameter drift (e.g. increasing excitability, potentially linked to extracellular K^+ accumulation) pushing the system past a saddle-node bifurcation → abrupt transition to a high-activity state
- Stimulation-induced state changes: in this framework, a brief deep brain stimulation (DBS) or transcranial electrical stimulation (TES) pulse can push the system across a basin boundary → lasting effect without continuous stimulation

Key message: bifurcation analysis doesn't just describe what CAN happen — it predicts what triggers *transitions and what* maintains *them. Foundation for Part III (epilepsy).*

Stochastic NMMs: Noise as a Feature

Real neural populations are finite (N ≈ 10^3–10^5 per cortical column); fluctuations physiologically meaningful.

Two noise sources:

Additive: $\tau \frac{dE}{dt} = f(E,I) + \sigma_{ext}\xi(t)$: background synaptic bombardment from other regions; state-independent.

Multiplicative (finite-size): $\tau dE/dt = f(E,I) + \left(1/\sqrt{N}\right) \cdot g(E,I)\xi(t)$. As an example, binomial binary-activity intuition gives $g \propto \sqrt{\mathrm{E}(1-\mathrm{E})}$ [22].

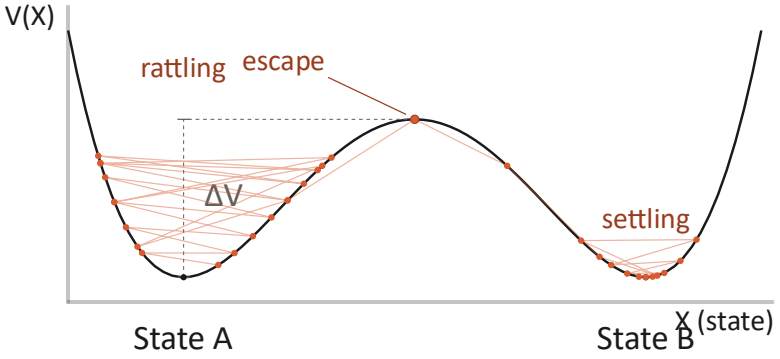

Noise-driven transitions between attractors:

In a bistable NMM, noise occasionally kicks the system from one attractor to another. Because Wilson–Cowan systems are generally non-gradient (no strict scalar potential V), mean escape times follow an exponential dependence on a barrier / noise scale:

$$T_{\mathrm{escape}} \sim \exp(\Delta V / D)$$

E, I	excitatory / inhibitory population activity
f(E, I)	deterministic Wilson–Cowan drift
τ	population time constant
ξ(t)	Gaussian white noise, ⟨ξ(t)ξ(t')⟩ = δ(t−t')
σ_ext	external (additive) noise amplitude
N	population size (number of neurons)
g(E, I)	state-dependent noise amplitude (finite-size)
V(X)	quasi-potential along reaction coordinate X
ΔV	barrier height between attractors
D	effective noise intensity (∝ σ²)
T_escape	mean first-passage time between attractors

Clinical relevance: absence seizures (brief, sudden loss of consciousness without convulsions) may reflect noise-driven transitions in a bistable thalamocortical NMM [23]; noise also explains trial-to-trial variability in stimulation responses.

Stochastic NMMs: Numerical Integration

General Itô SDE: $dX = f(X)dt + g(X)dW$ [5]

X_j	state at step j
Δt	integration time step
f(X)	drift coefficient (deterministic part)
g(X)	diffusion coefficient (noise amplitude)
g'(X) = dg/dX	derivative of diffusion w.r.t. state
ΔW_j	Wiener increment over $[t_j, t_{j+1}]$
ξ_j	standard normal draw, $\mathcal{N}(0, 1)$

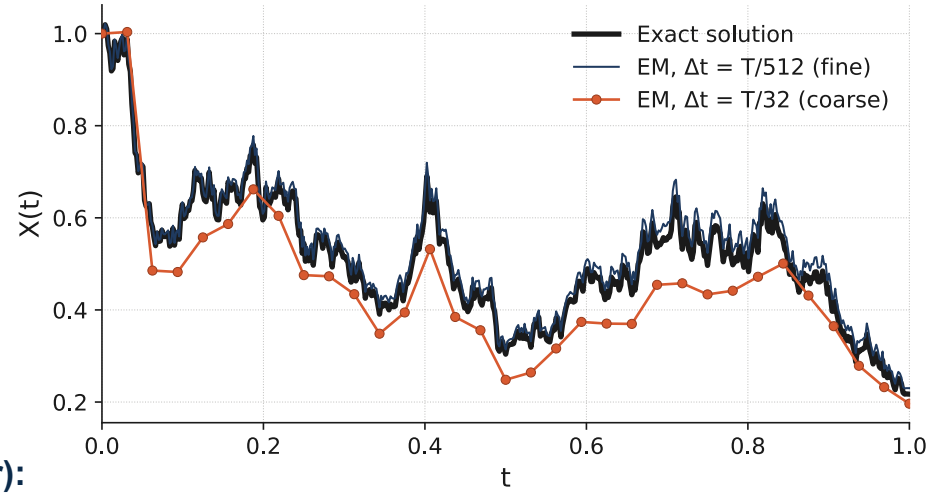

Linear SDE dX = λX dt + μX dW, λ = 2, μ = 1, X_0 = 1. Both EM solutions driven by the same Brownian path W.

Euler–Maruyama (stochastic analog of forward Euler):

$$X_{j+1} = X_j + f(X_j)\Delta t + g(X_j)\Delta W_j, \quad \Delta W_j = \sqrt{\Delta t}\,\xi_j, \quad \xi_j \sim \mathcal{N}(0,1)$$

Milstein correction
(scalar / commutative-noise version, multiplicative noise):

$$X_{j+1} = X_j + f\,\Delta t + g\,\Delta W_j + (1/2)\,g g'\left[(\Delta W_j)^2 - \Delta t\right]$$

Strong vs. weak convergence: strong = pathwise accuracy (first-passage times, transition rates); weak = accuracy of moments and distributions (ensemble averages).

Heuristic rule of thumb: Δt ≤ 0.1 × (smallest time constant in the NMM). For Jansen–Rit with $\tau_e = 10$ ms: Δt ≤ 1 ms. For stochastic problems, stability and accuracy also depend on noise strength and on the observable of interest.

Part II Summary: Landscape of Dynamic States

The Wilson–Cowan system, analyzed with the same phase-plane tools from W02, reveals a rich landscape of stable states, oscillations, bistability, and hysteresis, all controlled by a few parameters (connection weights, external drive). Different bifurcation types produce qualitatively different dynamics. Noise drives transitions between coexisting states.

Next: we will see that epilepsy maps directly onto this framework: seizure onset and offset are bifurcations, and different seizure types correspond to different bifurcation pairs [6, 10].

Outline for Today

- From spikes to populations: Mean-field reduction, Wilson–Cowan, Jansen–Rit, the NMM zoo
- Bifurcation analysis & stochastic dynamics: Phase plane, bifurcation types, hysteresis, stochastic NMMs, SDE numerics
- **Epilepsy as a dynamical disease: Seizures as bifurcations, Saggio taxonomy, Epileptor, Virtual Epileptic Patient, closed-loop control**
- Whole-brain models: Structural connectivity, region- and surface-based models, The Virtual Brain, subject-specific predictions
- Hybridization: Bridging scales; the IT'IS/Jirsa pipeline for personalized non-invasive brain stimulation [1]
- Exercise session: Prof. Niels Kuster guest lecture: “Coexistence & Synergy: Basic Research, Innovations, and Spin-Offs at Z43”

Seizures are Bifurcations

Epilepsy as a 'dynamical disease' [24]: smooth changes in a control parameter drive the brain across a bifurcation

The mapping

- Bifurcation parameter → excitability (channel mutations), E/I ratio (GABAergic deficit), extracellular K^+, external drive (reflex triggers)
- Normal state = stable fixed point of the NMM
- Seizure = limit cycle / bursting attractor
- Seizure onset = bifurcation crossing (parameter drifts past a critical value)
- Seizure offset = reverse transition, possibly a different bifurcation type than onset

Three canonical transition mechanisms [23]

1. Noise-induced escape between coexisting attractors
   - Absence seizures — bistable model
2. Slow parameter drift past a bifurcation
   - Temporal lobe epilepsy — excitability gradually increases
3. Stimulus-triggered jump across a basin boundary
   - Reflex (photosensitive) epilepsy

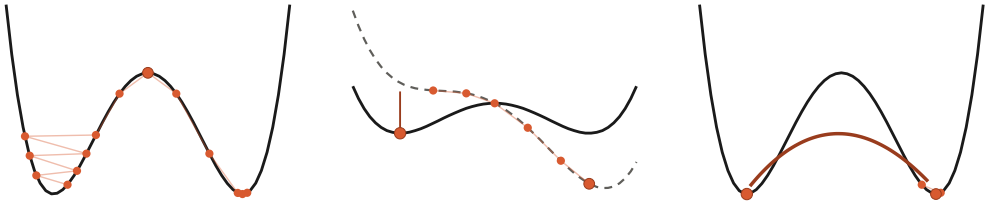

(a) Noise
random kicks across the barrier
absence seizures

(b) Drift
parameter slowly reshapes the landscape
temporal lobe epilepsy

(c) Stimulus
a single push across the basin boundary
photosensitive epilepsy

Taxonomy of Seizure Dynamotypes

Saggio & Jirsa: 4 onset × 4 offset bifurcations → 16 dynamotypes, derived from theory [25] and validated in patients

Onset bifurcations

Type	Electrographic signature
Saddle-node	Abrupt amplitude jump + DC shift
SNIC	Frequency approaches zero continuously at onset
Supercrit. Hopf	Gradual amplitude increase (small → large)
Subcrit. Hopf	Abrupt amplitude onset (discontinuous jump)

Offset bifurcations

Type	Electrographic signature
Saddle-homoclinic	Logarithmic ISI scaling → 0 Hz (slowing)
SNIC	Square root-frequency scaling → 0 Hz
Supercrit. Hopf	Gradual amplitude decrease
Fold limit cycle	Abrupt cessation (amplitude → 0)

Empirical validation: analysis of >2,000 focal-onset seizures found evidence for all 16 predicted dynamotypes [10]. The dominant combination is saddle-node onset / saddle-homoclinic offset ('square-wave bursting'). Individual patients can exhibit multiple dynamotypes across recorded seizures.

Epileptor Model

***Key parameter: x_0 (excitability)**
Inferred per-region in patient-specific Virtual Epileptic Patient (VEP) (next slide).

Jirsa et al. 2014 [6]: a 5-variable, two-timescale phenomenological NMM for seizure dynamics

Fast subsystem (tonic-like, x_1/y_1)

$$\frac{dy_1}{dt} = y_0 - 5x_1^2 - y_1$$
$$\frac{dx_1}{dt} = y_1 - f_1(x_1, x_2) - z + I_{ext1}$$

Slow permittivity variable (z)

$$\frac{dz}{dt} = \frac{1}{\tau_0}(4(x_1 - x_0) - z), \quad \tau_0 \approx 2857$$

Slow subsystem (spike-wave, x_2/y_2)

$$\frac{dy_2}{dt} = \frac{1}{\tau_2}(-y_2 + f_2(x_2))$$
$$\frac{dx_2}{dt} = -y_2 + x_2 - x_2^3 + I_{ext2} + 2g(x_1) - 0.3(z - 3.5)$$

Observable output

$\psi = x_1 + x_2$
local field potential (LFP) / stereoelectroencephalography (SEEG) proxy

Piecewise-defined nonlinearities

f_1, f_2, and $g(x_1)$ are piecewise: the 5-variable ODE skeleton alone does NOT capture seizure dynamics; the functional forms are essential.

Dynamical structure

- Slow evolution of z drives the fast subsystem across onset and offset bifurcations
- Canonically: saddle-node at onset, saddle-homoclinic at offset [6]
- Autonomous switching between ictal (during seizures) and interictal states (between seizures); seizures self-terminate [26]

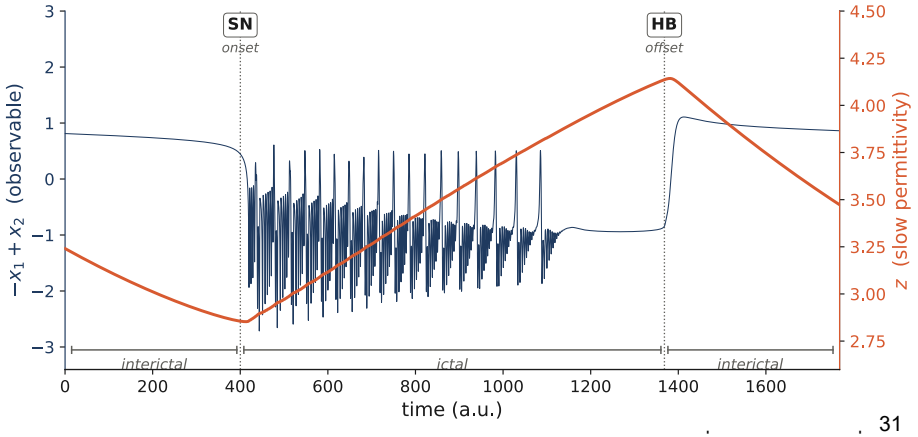

The Virtual Epileptic Patient

Individual structural connectomes + Epileptor nodes → patient-specific surgical planning

Pipeline

1. Patient MRI / diffusion-weighted imaging (DWI) → structural connectivity matrix (162 regions, VEP atlas)
2. Each region = an Epileptor node, coupled via permittivity coupling on the slow timescale; regional excitability $x_{0,i}$ is the key free parameter per region
3. High values of $x_{0,i}$ mark the epileptogenic zone (EZ)
4. Bayesian inference fits x_0 to SEEG recordings → probabilistic EZ map
5. Predicted EZ compared with clinical hypothesis → informs resection boundaries

Clinical evidence

Wang et al. 2023 [8] — 53 drug-resistant epilepsy patients:

- EZ precision ≈ 0.6
- Seizure-free patients: false discovery rate (FDR) of 0.028
- Non-seizure-free: FDR of 0.407 (was it *really* false discovery?...)

EPINOV (NCT03643016)

Ongoing large multicenter randomized trial, ~356 planned participants across 11 French centers — largest prospective test of computational modeling for epilepsy surgery [27].

→ The most advanced clinical validation to date of any whole-brain computational model.

The Virtual Epileptic Patient

MAKHALOVA ET AL. Epilepsia® 1951

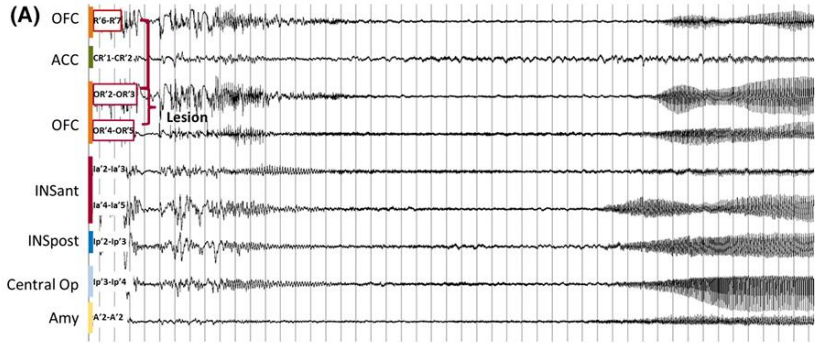

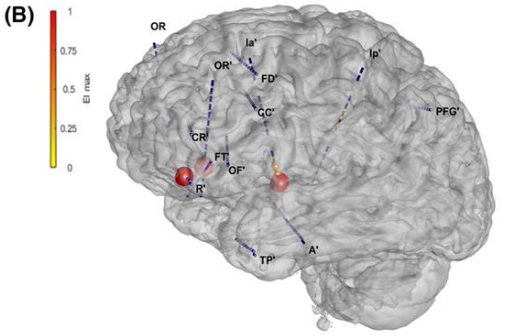

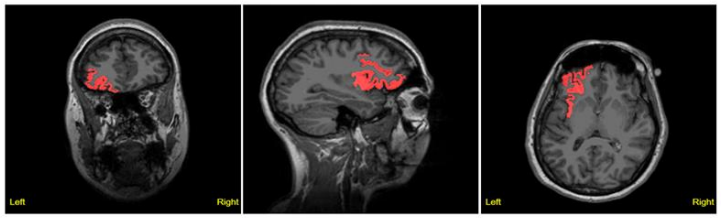

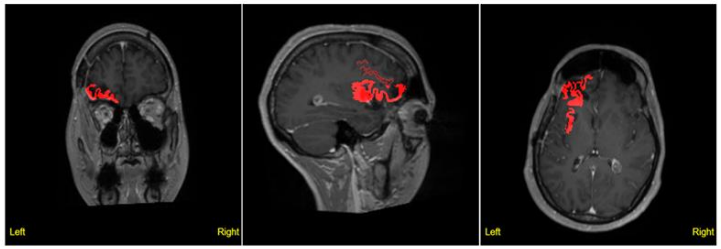

(D)

Brain regions	EZ_{VEP}	EV
Left-Insula-gyri-brevi	Yes	1
Left-Orbito-frontal-cortex	Yes	0.835
Left-Inferior-frontal-sulcus	Yes	0.53

Illustrative VEP case: 29-year-old woman with drug-resistant focal seizures. From SEEG (A) and the personalized network model (B), VEP inferred an epileptogenic zone spanning left insula, orbitofrontal cortex, and inferior frontal sulcus (C, D). Surgery resected the first two regions (E); seizures relapsed, and follow-up localized residual activity to unresected inferior frontal sulcus — the region VEP had flagged but the clinical hypothesis missed. Adapted from Makhalova et al., *Epilepsia* 2022.

Closed-Loop Seizure Control: NeuroPace RNS

The clinical embodiment of bifurcation control — previewed in W01, now in the NMM framework

The NeuroPace Responsive Neurostimulation (RNS) System (FDA 2013) continuously monitors intracranial electrocorticography (ECoG), detects seizure onset, and delivers brief stimulation pulses to abort the seizure — intervening near the bifurcation boundary before the system fully commits to the ictal attractor.

Connection to our framework

- Detection = identifying approach to a bifurcation (biomarker threshold crossing)
- Intervention = pushing the system back across the basin boundary (brief stimulation)
- Same detect–respond–optimize paradigm as adaptive DBS (W07 slides 34–36), but for epilepsy
- 75% median seizure reduction at 9 years Nair et al. 2020 [28].

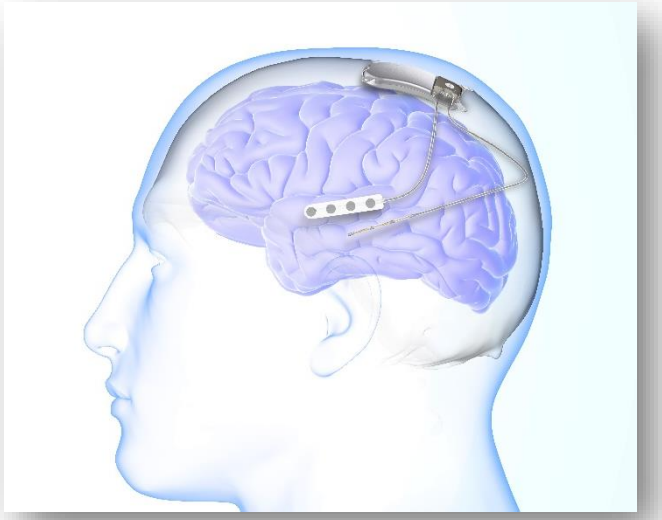

Looking forward

Can VEP models predict which stimulation parameters will most effectively abort seizures in a given patient? The optimization question connects to W11.

Part III Summary: Epilepsy as a Dynamical Disease

- Seizure dynamics map directly onto the bifurcation framework from Part II — onset and offset are transitions between attractors of an NMM.
- The Saggio/Jirsa taxonomy predicts 16 dynamotypes; all have been observed in >2,000 focal-onset seizures (square-wave bursting dominant).
- The Epileptor captures the essential two-timescale dynamics with 5 variables and piecewise nonlinearities; slow z drives fast subsystem across bifurcations.
- Embedded in a patient-specific connectome (VEP), it yields clinically actionable predictions — validated in 53 patients, prospective trial in ~356.
- Closed-loop RNS is the clinical realization of intervening near a bifurcation — same paradigm as adaptive DBS, connects forward to W11.

→ Next: scaling up from single-node dynamics to whole-brain network models

Outline for Today

- From spikes to populations: Mean-field reduction, Wilson–Cowan, Jansen–Rit, the NMM zoo
- Bifurcation analysis & stochastic dynamics: Phase plane, bifurcation types, hysteresis, stochastic NMMs, SDE numerics
- Epilepsy as a dynamical disease: Seizures as bifurcations, Saggio taxonomy, Epileptor, Virtual Epileptic Patient, closed-loop control
- **Whole-brain models: Structural connectivity, region- and surface-based models, The Virtual Brain, subject-specific predictions**
- Hybridization: Bridging scales; the IT'IS/Jirsa pipeline for personalized non-invasive brain stimulation [1]
- Exercise session: Prof. Niels Kuster guest lecture: “Coexistence & Synergy: Basic Research, Innovations, and Spin-Offs at Z43”

Single Nodes → Brain Networks

Parcellate → assign an NMM per region → couple via structural connectivity and delays [29, 30, 31]

$$\frac{dx_i}{dt} = F(x_i) + G\sum_j C_{ij}\, h\left(x_j\left(t-\tau_{ij}\right)\right) + \eta_i(t)$$

Three ingredients

1. Local dynamics $F(x_i)$ — the NMM at each node; sets the intrinsic oscillatory repertoire.

2. Structural connectivity C_{ij} — the wiring diagram (which regions talk, with what strength).

3. Conduction delays $\tau_{ij} = L_{ij}/v$ — tract length / axonal velocity (typically 5–20 m/s, often fit as an effective parameter rather than measured directly); sets inter-regional phase.

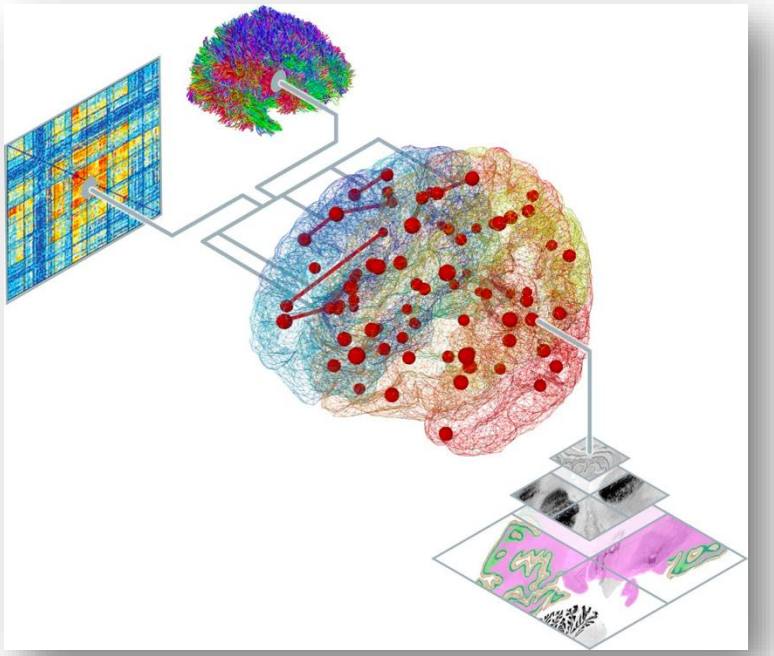

The global coupling "G"

Most important free parameter (typically). Optimal fits to empirical functional connectivity (FC) consistently occur near a critical point (bifurcation) — noise-driven fluctuations explore a rich repertoire shaped by structure [32].

Image: www.ebrains.eu

Structural Connectivity from Diffusion MRI

DWI → tractography → C_{ij}, with streamline count as the coupling-weight proxy

Standard parcellations

- Desikan–Killiany: 68 regions [13]
- Schaefer: 100–1000 functional parcels [33]
- Glasser Human Connectome Project Multi-Modal Parcellation (HCP-MMP): 360 multimodal parcels [34]

Despite their limitations, structure-derived connectomes consistently constrain whole-brain dynamics better than random / shuffled matrices.

**Note on terminology*:
- **DWI** (diffusion-weighted imaging) is the acquisition
- **DTI** (diffusion tensor imaging) is one possible model fit to DWI data, yielding a rank-2 tensor per voxel.
- Tractography can use DTI or more modern models (constrained spherical deconvolution, q-ball); anisotropic conductivity tensors (W11) require the tensor fit.

Critical caveats

- Crossing fibers: 60–90% of white matter (WM) voxels contain crossing fibers unresolvable by DTI
- False positives dominate — ISMRM** Tractography Challenge showed more invalid than valid bundles [35]
- Connections typically treated as **undirected;** directionality not recovered directly
- Distance-dependent attrition: long-range connections underrepresented

**International Society for Magnetic Resonance in Medicine

Note: DTI also yields anisotropic conductivity tensors for EM simulation — that's W11 (Esra). Here: topology only.

Structural Connectivity from Diffusion MRI

DWI → tractography → C_{ij} ,with streamline count as the coupling-weight proxy

Standard parcellations

- Desikan–Killiany: 68 regions [13]
- Schaefer: 100–1000 functional parcels [33]
- Glasser Human Connectome Project Multi-Modal Parcellation (HCP-MMP): 360 multimodal parcels [34]

Despite these limitations, structure-derived connectomes consistently constrain whole-brain dynamics better than random / shuffled matrices — the structural scaffold matters.

**Note on terminology*:
- **DWI** (diffusion-weighted imaging) is the acquisition
- **DTI** (diffusion tensor imaging) is one model fit to DWI data, yielding a rank-2 tensor per voxel.
- Tractography can use DTI or more modern models (CSD, q-ball); anisotropic conductivity tensors (W11) require the tensor fit.

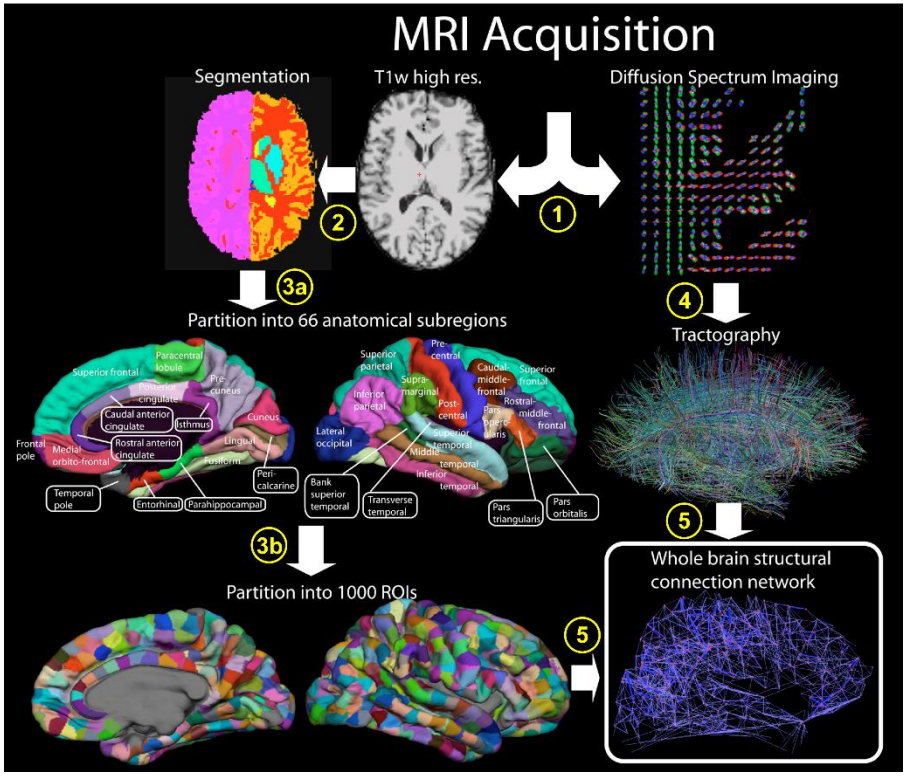

Hagmann P et al. (2008) Mapping the Structural Core of Human Cerebral Cortex. PLoS Biol 6(7): e159. https://doi.org/10.1371/journal.pbio.0060159

Note: DTI also yields anisotropic conductivity tensors for EM simulation — that's W11 (Esra). Here: topology only.

(Dynamic) Functional Connectivity

- **Static Functional Connectivity (FC):** Measures time-averaged, pairwise correlations between regions across an entire session.
  - *Limitation:* Assumes a stationary network; masks transient shifts in coordination.
- **Functional Connectivity Dynamics (FCD):** Quantifies how large-scale network synchronization patterns evolve over time.
  - *Method:* Typically uses a "sliding window analysis" to extract time-resolved connectivity matrices.

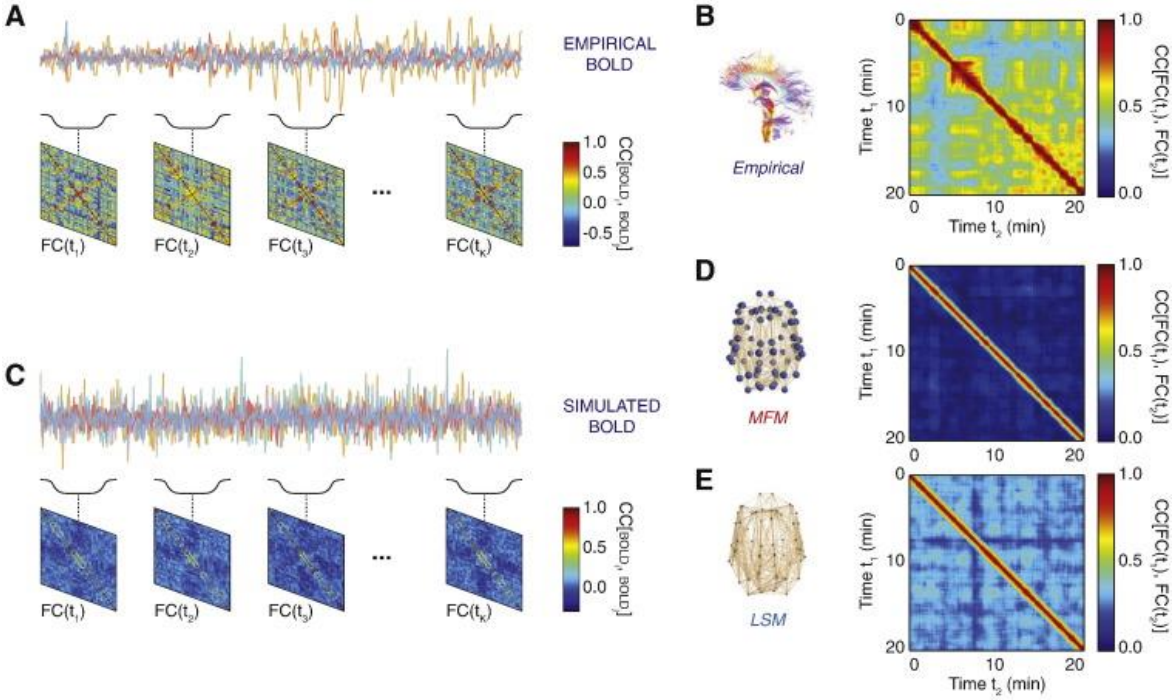

- **Metastability Visualization:** FCD matrices reveal the brain's continuous switching between distinct, transiently stable network configurations.
  - *Significance for modeling:* Whole-brain models are fitted to maximize their *FCD repertoire*, ensuring the *in silico* brain can access the same range of states as the *in vivo* brain.

Image adapted from Hansen et al., *NeuroImage* 105 (2015).

Region- vs. Surface-Based Models

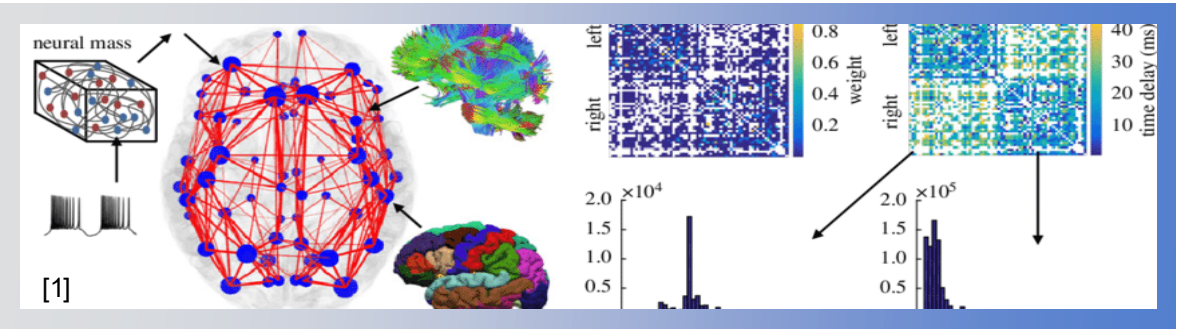

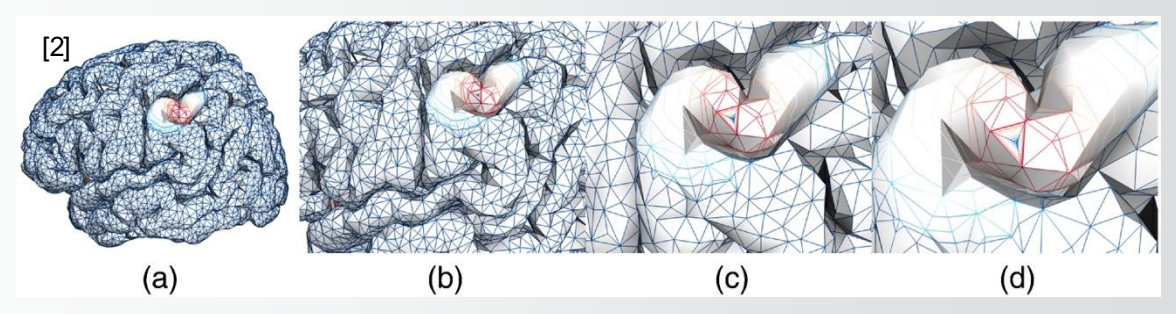

region
- parcellation → NMM
- global connectivity only
- low resolution (low runtime)

surface
- cortical mesh
- global and local connectivity
- high resolution (high runtime w/o optimization)

[1] Spase Petkoski, Phil. Trans A. (2019)
[2] Sanz-Leon et al., NeuroImage (2015)

Region-Based Whole-Brain Models

One NMM per parcellated region → coupled ODE system. Tractable and widely used. Example: 68 regions (Desikan–Killiany) × 6 ODEs (Jansen–Rit) = 408 coupled equations; seconds on a laptop.

Common NMM choices for whole-brain modeling

Model	Variables	Notes
Reduced Wong–Wang	2 / node	Bistability from NMDA recurrence; Deco 2013
Hopf normal form	2 / node	Minimal oscillator near a bifurcation
Jansen–Rit	6 / node	Realistic EEG spectra; standard for forward modeling
Epileptor	5 / node	Seizure dynamics (Part III)
Wilson–Cowan	2 / node	Analytical work & bifurcation studies

Model choice trades off computational cost, biological fidelity, and fit target: 2-variable reductions (Hopf, reduced Wong–Wang) dominate FC fitting because they run fast over wide parameter sweeps [31]; 6-variable Jansen–Rit is preferred when the observable is EEG spectra [3, 18].

Fitting & validation workflow

- Step 1 — static FC: Pearson correlation of regional blood-oxygen-level-dependent (BOLD) or band-limited EEG power. Structure-derived connectomes consistently outperform randomized/shuffled matrices [29, 30, 31, 36].
- Step 2 — FCD: sliding-window FC correlation matrix captures non-stationary dynamics and metastability [37] that static FC averages away. Whole-brain models operate near a bifurcation/edge-of-criticality point where this metastable repertoire is maximized.

Surface-Based Models & Neural Fields

Continuous neural-field equation on the cortical surface mesh — richer spatial dynamics, higher cost [38, 39]

$$\tau \frac{\partial u(x,t)}{\partial t} = -u(x,t) + \int_{\Omega} w(x,y), f\big(u(y,t)\big), dy + I_{ext}(x,t)$$

where w(x, y) is the connectivity kernel — often, though not always, modeled with a Mexican-hat-type kernel (local excitation, lateral inhibition) — and f is a sigmoidal firing-rate function.

Richer spatial dynamics

- Traveling waves [40]
- Stationary bumps
- Spiral waves
- Turing patterns

…region-based models do not capture continuous cortical-sheet dynamics / wavefront geometry.

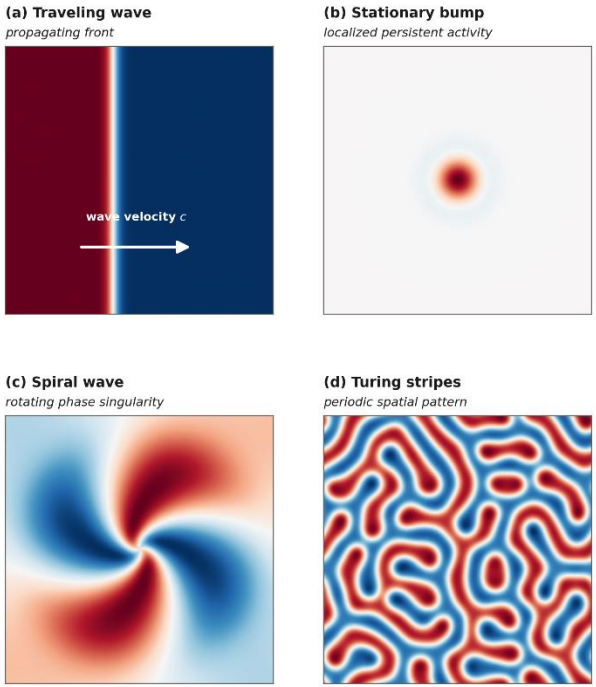

Cost & relevance

- ~10^4–10^5 cortical surface vertices
- Orders of magnitude more expensive than region-based models
- Epilepsy relevance: seizure propagation often involves traveling waves on the cortical surface — surface-based models can capture this wavefront propagation.

The Virtual Brain (TVB) Platform

Stay tuned for "BraiNN", an exciting new JAX-based simulation tool soon to be released by IT'IS...

The leading open-source platform for whole-brain simulation [11, 42]

Built-in components

- Standard connectomes: e.g. HCP; patient-specific from DWI
- Multiple NMM options (Jansen–Rit, W–C, Wong–Wang, Epileptor, Hopf, Fitzhugh-Nagumo (FHN), Kuramoto)
- Forward models for simulated EEG/MEG (lead-field matrices explained in W09) and BOLD (Balloon–Windkessel hemodynamics)
- Parameter space exploration tools
- Deployed on EBRAINS cloud infrastructure [43]

Recent developments (2022–2026)

- TVB-NEST multiscale co-simulation: spiking-network regions within mean-field whole-brain models
- JAX-based gradient computation for rapid model fitting (TVB-Optim, a recent software development / preprint-era tool, not yet an established peer-reviewed component)
- Simulation-based inference for virtual brain models of disorders [41]

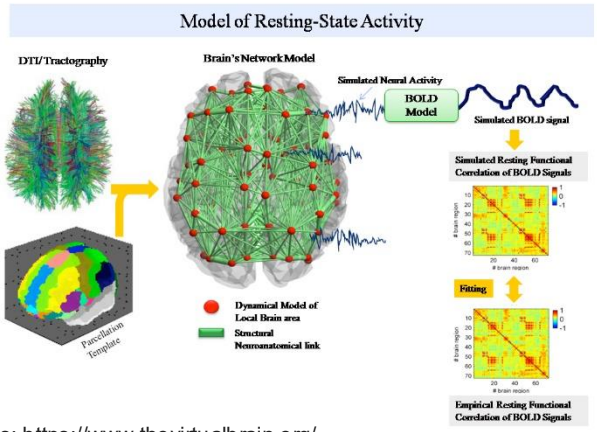

Images: https://www.thevirtualbrain.org/

Subject-Specific Predictions

Individual DTI + fitted NMMs →
predict intervention outcomes per patient

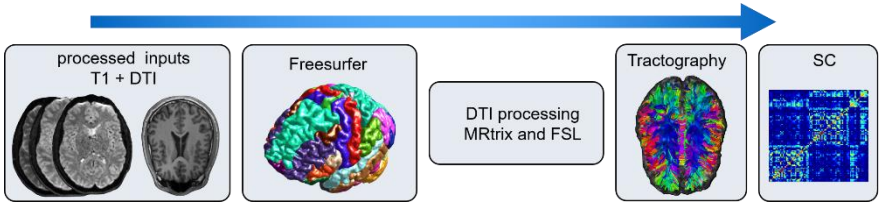

Application domains

- Epilepsy surgery (VEP, Part III): predict seizure propagation → inform resection boundaries
- Stroke recovery: predict functional reorganization after lesion → optimize rehabilitation targets
- Stimulation targeting: predict brain-wide effects of local stimulation → optimize electrode placement and parameters (bridge to Part V)

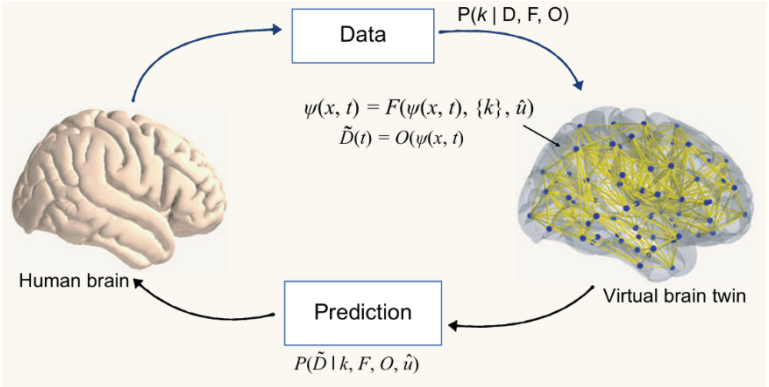

Huifang E Wang et al., Virtual brain twins: from basic neuroscience to clinical use, *National Science Review*, Volume 11, Issue 5, May 2024

Model inversion approaches (more optimization in W11)

Grid search · Bayesian optimization · approximate Bayesian computation (ABC) · deep-learning-based simulation-based inference (amortized inference)

Bottleneck: model inversion cost is currently the main obstacle to clinical deployment.

Application-Specific Predictions

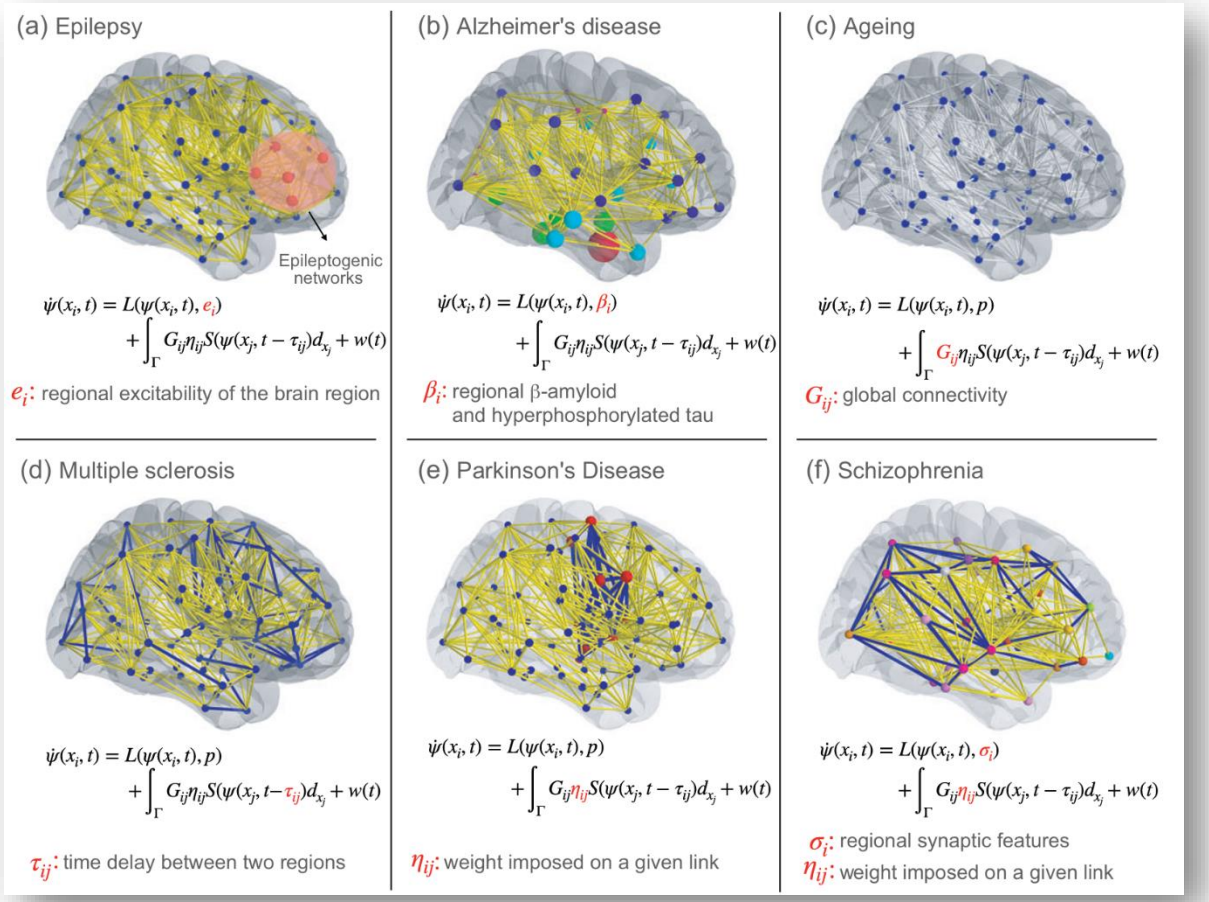

Huifang E Wang et al., Virtual brain twins: from basic neuroscience to clinical use, *National Science Review*, Volume 11, Issue 5, May 2024

Part IV Summary

Whole-brain models: NMM nodes on a structural scaffold

- Whole-brain models embed NMM nodes in DTI-derived structural connectomes, producing simulated brain dynamics comparable to empirical EEG / fMRI.
- Region-based models offer tractability; surface-based neural-field models offer spatial richness (traveling waves, Turing patterns) at substantially higher cost.
- The Virtual Brain (TVB) provides an open-source infrastructure — NMMs, connectomes, forward models, parameter exploration — on EBRAINS.
- Clinical validation is most advanced for epilepsy (VEP / EPINOV); other applications (stroke, stimulation targeting) are at earlier maturity.
- Critical gap: these models are phenomenological — they cannot represent the biophysical specificity of neurostimulation. That's the problem Part V addresses.

→ Next: hybridization — bringing biophysical E-field models into the phenomenological scaffold

Outline for Today

- From spikes to populations: Mean-field reduction, Wilson–Cowan, Jansen–Rit, the NMM zoo
- Bifurcation analysis & stochastic dynamics: Phase plane, bifurcation types, hysteresis, stochastic NMMs, SDE numerics
- Epilepsy as a dynamical disease: Seizures as bifurcations, Saggio taxonomy, Epileptor, Virtual Epileptic Patient, closed-loop control
- Whole-brain models: Structural connectivity, region- and surface-based models, The Virtual Brain, subject-specific predictions
- **Hybridization: Bridging scales; the IT'IS/Jirsa pipeline for personalized non-invasive brain stimulation [1]**
- Exercise session: Prof. Niels Kuster guest lecture: “Coexistence & Synergy: Basic Research, Innovations, and Spin-Offs at Z43”

The Multi-Scale Gap

NMMs are macroscopic — but interventions act at the microscale.

What biophysical models capture

- FEM electric fields (stimulation & sensing) (W04)
- Cable eqns & activating fn (W03)
- Compartmental neurons (W07)
- Ion-channel dynamics (W05)
- But: intractable at whole-brain scale

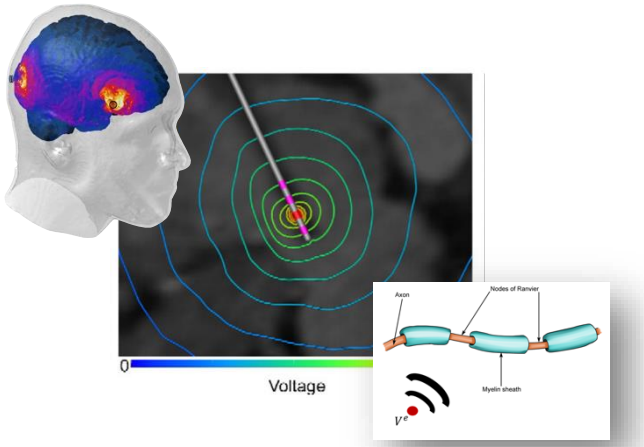

What NMMs cannot represent

- DBS electrode E-field in subthalamic nucleus (STN)
- Morphology-dependent polarization (transcranial direct current stimulation; tDCS)
- Ion-channel kinetics under drugs
- Axon geometry, myelination, gradients
- Skull/CSF/folding effects on fields

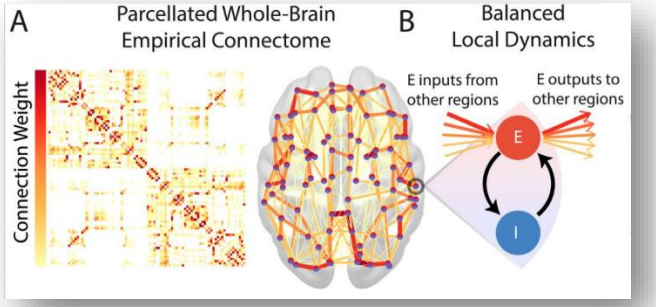

→ How do we predict whole-brain effects of a local, biophysically specific intervention?

Herzog R et al., Neural mass modeling for the masses: Democratizing access to whole-brain biophysical modeling with FastDMF. *Netw Neurosci.* 2024 Dec 10;8(4):1590-1612. doi: 10.1162/netn_a_00410. PMID: 39735506; PMCID: PMC11674928.

Hybridization Strategy

Detailed biophysics where it matters; NMMs everywhere else.

Three approaches (D'Angelo & Jirsa 2022) [44]

1. Full multiscale everywhere — intractable today
2. Multiscale-minded hybrid — detailed node(s) at intervention site, NMMs elsewhere: sweet spot
3. Brute-force microscale — awaits exascale computing (though BBP tried ☺)

Existing implementations

- TVB–NEST co-simulation [45]
- Meier et al. 2022: virtual DBS (ANNarchy+TVB) [46]
- Merlet et al. 2013: realistic head + neural population model + transcranial current stimulation (tCS)-to-EEG hybrid pipeline [51]

Practical architecture

- Phenomenological nodes: NMMs for most regions
- Biophysical node(s): spiking/compartmental at stim site
- Interface: firing rate ↔ NMM coupling

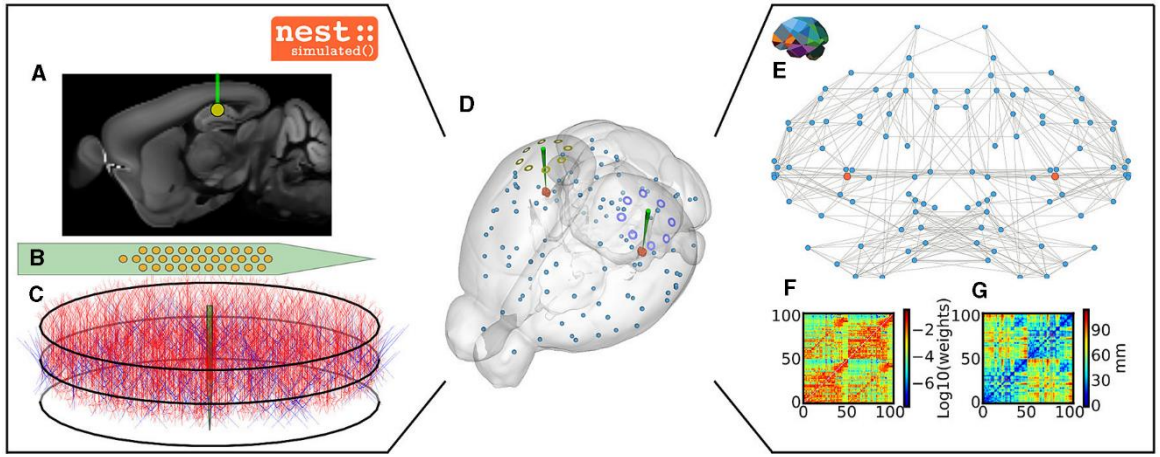

Kusch L et al., (2024) Multiscale co-simulation design pattern for neuroscience applications. *Front. Neuroinform.* 18:1156683. doi: 10.3389/fninf.2024.1156683

Coupling E-Fields into Network Dynamics ($\lambda \cdot \mathrm{E}$)

The coupling assumption

- Nodes are Jansen–Rit (or other) NMMs; edges remain DWI-derived structural connectivity (C_{ij} unchanged by stimulation).
- Personalized FEM E-field is projected onto the cortical normal at each node.
- The term $\lambda \cdot E_{\perp}$ is added as a perturbation to the mean pyramidal-cell membrane potential in that node.
- Acts on pyramidal cells only; interneuron effects neglected (modest per [49]).

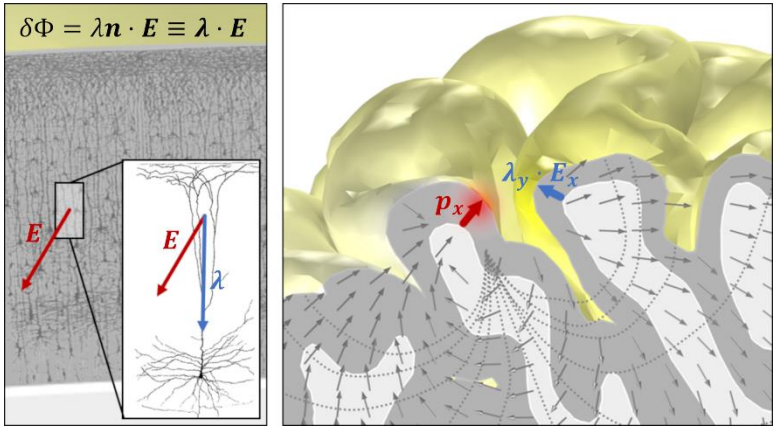

What this is — and isn't

- A phenomenological coupling guess, not a derived reduction. The functional form is a modeling choice, validated empirically.
- Well-motivated for transcranial alternating current stimulation (tACS)/tDCS, where quasi-static fields linearly shift membrane potential.
- An open question for temporal interference stimulation (TIS), low-intensity focused ultrasound (LIFUS), and other modalities whose coupling mechanisms are less settled.
- Early neural-mass / tCS coupling examples: Molaee-Ardekani et al. (2013) [49]; tCS modeling frameworks reviewed by Ruffini et al. (2013) [50]; Karimi et al. (2025) [1] adopts related phenomenological $\lambda E_{\perp}$ coupling.

$$V_{\mathrm{pyr}} \rightarrow V_{\mathrm{pyr}} + \lambda \mathbf{E} \cdot \hat{\mathbf{n}}$$

λ: effective membrane space constant (tuned against empirical signals)

Ruffini G et al., (2020) Realistic modeling of mesoscopic ephaptic coupling in the human brain. *PLoS Comput Biol* 16(6): e1007923. https://doi.org/10.1371/journal.pcbi.1007923

The Karimi et al. Pipeline

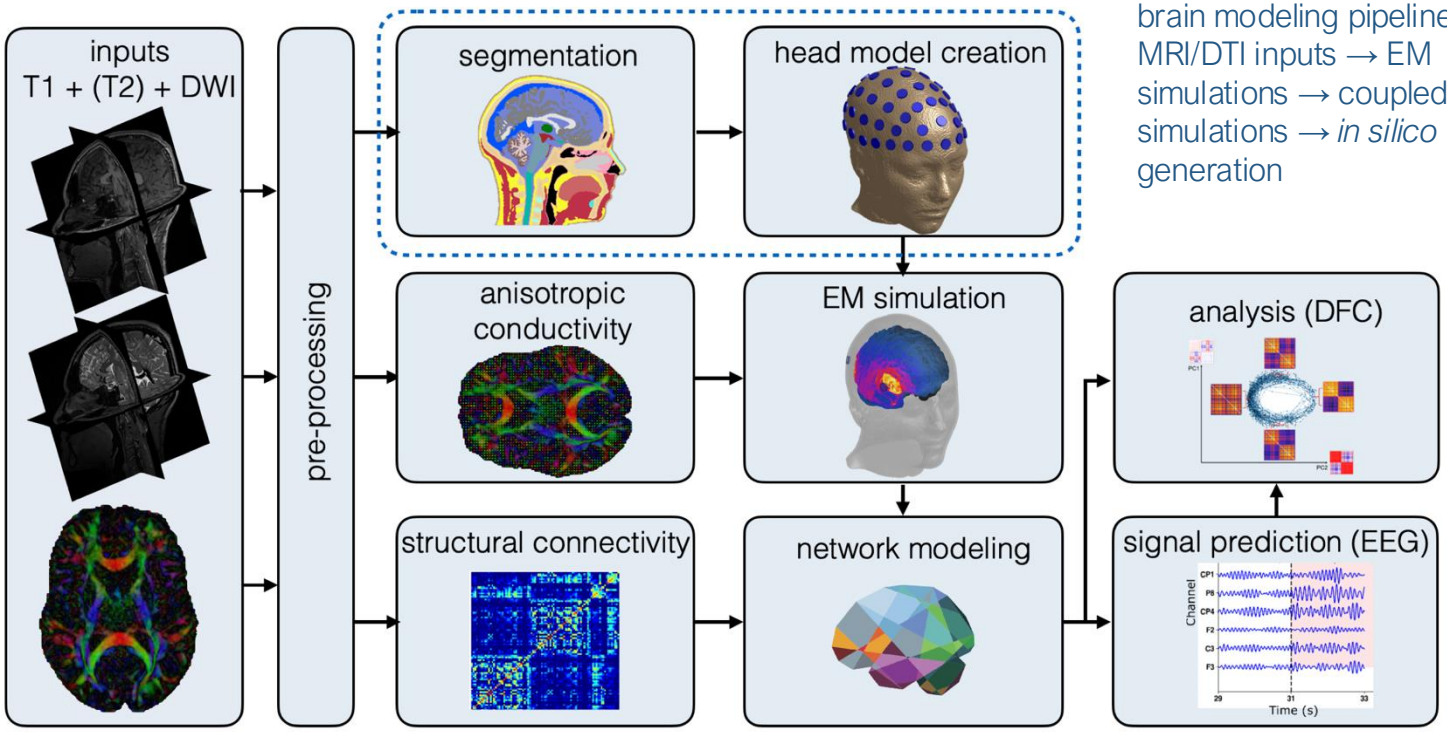

brain modeling pipeline - MRI/DTI inputs → EM simulations → coupled network simulations → *in silico* signal generation

- coupling NMM-based description of brain activity to EM stimulation input closes the loop between stimulus and response → advanced/personalized tES schemes; effect-driven
- lead field matrix personalization
- EM exposure coupling control paradigms

The Karimi et al. Pipeline: Personalization

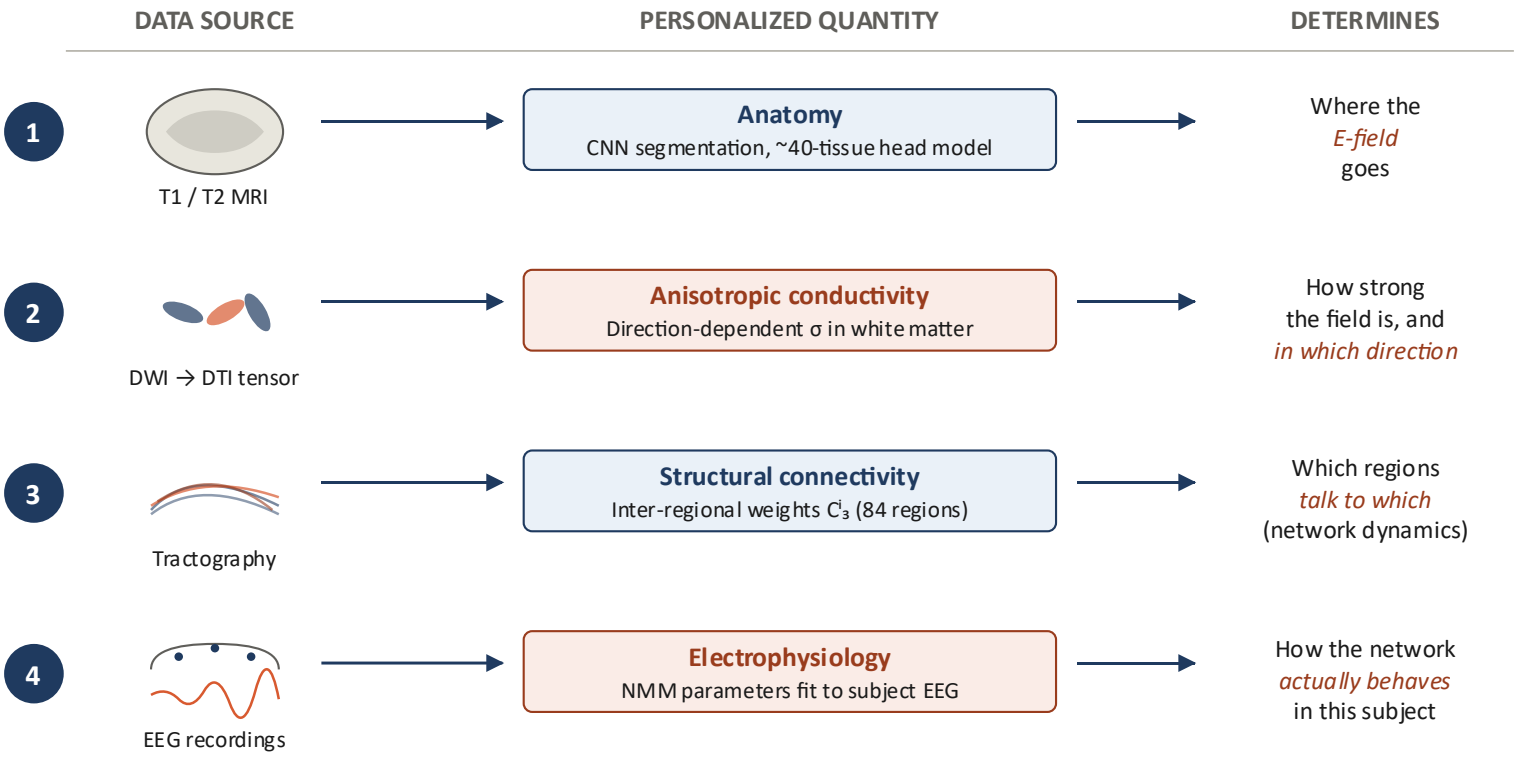

Toward "digital twins"

- A *virtual brain twin* is a personalized *in silico* model: MRI + DTI + (EEG) → subject-specific predictions, not population averages
- Query candidate stimulation protocols *before* the device is turned on
- Bottleneck is no longer forward simulation: it is *model inversion* fast enough for clinical timelines

The Karimi et al. Pipeline

Karimi et al. 2025, J. Neural Eng. 22:026061 [1]

A fully automated, modular personalized modeling pipeline on o²S²PARC.

Pipeline stages

- T1/T2 MRI + DWI → convolutional neural network (CNN) head segmentation (head40: up to 40 tissues).
- Personalized EM simulation: Sim4Life electro quasistatic-FEM (EQS-FEM); DWI-derived anisotropic WM conductivity.
- Structural connectivity from DWI tractography (Desikan–Killiany, 84 regions).
- Surface-based whole-brain J-R model (~20k cortical nodes); long-range coupling from personal structural connectivity (SC).
- Stimulation coupling: $\lambda E_{\perp}$perturbs pyramidal V_m at each node (slide 41).
- Virtual EEG via reciprocity-based lead-field matrix.
- Multi-goal exposure optimization (strength / selectivity / collateral) → TIP tool for TIS planning.

What the paper shows

- Proof-of-concept #1 — tACS at P7–P8 (8 Hz, 15 Hz): produces the expected peak near the stimulation frequency in the simulated EEG power spectral density (PSD), spatially concentrated near the electrodes.
- Proof-of-concept #2 — baseline (unstimulated) resting dynamics show physiologically plausible fluctuations between inter-hemispheric synchronized and desynchronized states.
- Personalized anatomy substantially changes predicted exposure metrics — particularly collateral exposure.
- Framed as a shift from exposure-based to response-driven non-invasive brain stimulation (NIBS) optimization.
- NOT patient-level outcome validation — authors explicitly place empirical validation outside the study's scope.

→ Integrates W03/W04/W06/W07/today — points to W09/W10/W11.

Key Takeaways

1. NMMs are principled reductions of spiking networks — explicit assumptions, explicit losses.

2. Bifurcation analysis reveals essential dynamics. Wilson–Cowan's parameter space is organized by SN, Hopf, homoclinic curves emanating from a BT organizing center.

3. Epilepsy maps onto bifurcation theory; Saggio/Jirsa 16 dynamotypes; Epileptor captures the two-timescale essence; VEP reaches clinical-grade prediction.

4. Whole-brain models embed NMMs in structural connectomes. TVB is a popular open platform; FC/FCD fitting used for validation and model tuning.

5. Hybridization can bridge the multi-scale gap; biophysical detail where the intervention acts, NMMs elsewhere.

6. Personalization/subject-specific models (anatomy, tissue properties, connectivity, electrophysiology) can enhance outcomes → necessary step towards “digital twins”.

Outline for Today

- From spikes to populations: Mean-field reduction, Wilson–Cowan, Jansen–Rit, the NMM zoo
- Bifurcation analysis & stochastic dynamics: Phase plane, bifurcation types, hysteresis, stochastic NMMs, SDE numerics
- Epilepsy as a dynamical disease: Seizures as bifurcations, Saggio taxonomy, Epileptor, Virtual Epileptic Patient, closed-loop control
- Whole-brain models: Structural connectivity, region- and surface-based models, The Virtual Brain, subject-specific predictions
- Hybridization: Bridging scales; the IT'IS/Jirsa pipeline for personalized non-invasive brain stimulation [1]
- **Exercise session: Prof. Niels Kuster guest lecture: "Coexistence & Synergy: Basic Research, Innovations, and Spin-Offs at Z43"**

References

[1] Karimi et al., J Neural Eng 22:026061, 2025.
[2] Wilson & Cowan, Biophys J 12:1, 1972.
[3] Jansen & Rit, Biol Cybern 73:357, 1995.
[4] Izhikevich, Dynamical Systems in Neuroscience, MIT Press, 2007.
[5] Higham, SIAM Rev 43:525, 2001.
[6] Jirsa, Stacey, Quilichini, Ivanov & Bernard, Brain 137:2210, 2014.
[7] Jirsa et al., NeuroImage 145:377, 2017.
[8] Wang et al., Sci Transl Med 15:eabp8982, 2023.
[9] Deco, Jirsa, Robinson, Breakspear & Friston, PLoS Comput Biol 4:e1000092, 2008.
[10] Saggio et al., eLife 9:e55632, 2020.
[11] Sanz Leon et al., Front Neuroinform 7:10, 2013.
[12] Herculano-Houzel, Front Hum Neurosci 3:31, 2009.
[13] Desikan et al., NeuroImage 31:968, 2006.
[14] Montbrió, Pazó & Roxin, Phys Rev X 5:021028, 2015.
[15] Wilson & Cowan, Kybernetik 13:55, 1973.
[16] Lopes da Silva et al., Kybernetik 15:27, 1974.
[17] Freeman, Mass Action in the Nervous System, 1975.
[18] David & Friston, NeuroImage 20:1743, 2003.
[19] Liley et al., Network 13:67, 2002.
[20] Borisyuk & Kirillov, Biol Cybern 66:319, 1992.
[21] Sanchez-Vives & McCormick, Nat Neurosci 3:1027, 2000.
[22] Bressloff, SIAM J Appl Math 70:1488, 2010.
[23] Lopes da Silva et al., Epilepsia 44 Suppl 12:72, 2003.
[24] Milton & Jung (eds), Epilepsy as a Dynamic Disease, Springer, 2003.
[25] Saggio, Spiegler, Bernard & Jirsa, J Math Neurosci 7:7, 2017.
[26] El Houssaini, Bernard & Jirsa, eNeuro 7:ENEURO.0485-18.2019, 2020.
[27] Jirsa et al., Lancet Neurol 22:443, 2023.
[28] Nair et al., Neurology 95:e1244, 2020.
[29] Honey et al., PNAS 104:10240, 2007.
[30] Ghosh et al., PLoS Comput Biol 4:e1000196, 2008.
[31] Deco et al., PNAS 106:10302, 2009.
[32] Breakspear, Nat Neurosci 20:340, 2017.
[33] Schaefer et al., Cereb Cortex 28:3095, 2018.
[34] Glasser et al., Nature 536:171, 2016.
[35] Maier-Hein et al., Nat Commun 8:1349, 2017.
[36] Deco et al., J Neurosci 33:11239, 2013.
[37] Hansen et al., NeuroImage 105:525, 2015.
[38] Amari, Biol Cybern 27:77, 1977.
[39] Coombes, Biol Cybern 93:91, 2005.
[40] Jirsa & Haken, Phys Rev Lett 77:960, 1996.
[41] Hashemi et al., Mach Learn Sci Technol 5:035019, 2024.
[42] Sanz-Leon et al., NeuroImage 111:385, 2015.
[43] Schirner et al., NeuroImage 251:118973, 2022.
[44] D'Angelo & Jirsa, Trends Neurosci 45:777, 2022.
[45] Kusch et al., Front Neuroinform 18:1156683, 2024.
[46] Meier et al., Exp Neurol 354:114111, 2022.
[47] Neufeld, Szczerba, Chavannes & Kuster, Interface Focus 3:20120058, 2013.
[48] Sanchez-Todo et al., NeuroImage 270:119938, 2023.
[49] Molaee-Ardekani et al., Brain Stimulation, 2013, 6 (1), pp.25-39.
[50] Ruffini et al., IEEE Trans Neural Syst Rehabil Eng. 2013 May;21(3):333-45.
[51] Merlet et al., PLoS One. 2013;8(2):e57330.